



Targeting of Cdc42 GTPase in regulatory T cells unleashes antitumor T-cell immunity

Khalid W Kalim,¹ Jun-Qi Yang,¹ Mark Wunderlich,¹ Vishnu Modur,¹ Phuong Nguyen,¹ Yuan Li,¹ Ting Wen,² Ashley Kuenzi Davis ,¹ Ravinder Verma,¹ Qing Richard Lu,¹ Anil G Jegga,³ Yi Zheng,¹ Fukun Guo ¹

To cite: Kalim KW, Yang J-Q, Wunderlich M, *et al.* Targeting of Cdc42 GTPase in regulatory T cells unleashes antitumor T-cell immunity. *Journal for ImmunoTherapy of Cancer* 2022;**10**:e004806. doi:10.1136/jitc-2022-004806

► Additional supplemental material is published online only. To view, please visit the journal online (<http://dx.doi.org/10.1136/jitc-2022-004806>).

KWK and J-QY are joint first authors.

YZ and FG are joint senior authors.

Accepted 11 October 2022



© Author(s) (or their employer(s)) 2022. Re-use permitted under CC BY-NC. No commercial re-use. See rights and permissions. Published by BMJ.

For numbered affiliations see end of article.

Correspondence to

Dr Fukun Guo;
fukun.guo@cchmc.org

Professor Yi Zheng;
yi.zheng@cchmc.org

ABSTRACT

Background Cancer immunotherapy has taken center stage in cancer treatment. However, the current immunotherapies only benefit a small proportion of patients with cancer, necessitating better understanding of the mechanisms of tumor immune evasion and improved cancer immunotherapy strategies. Regulatory T (Treg) cells play an important role in maintaining immune tolerance through inhibiting effector T-cell function. In the tumor microenvironment, Treg cells are used by tumor cells to counteract effector T cell-mediated tumor suppression. Targeting Treg cells may thus unleash the antitumor activity of effector T cells. While systemic depletion of Treg cells can cause excessive effector T-cell responses and subsequent autoimmune diseases, controlled targeting of Treg cells may benefit patients with cancer.

Methods Treg cells from Treg cell-specific heterozygous Cdc42 knockout mice, C57BL/6 mice treated with a Cdc42 inhibitor CASIN, and control mice were examined for their homeostasis and stability by flow cytometry. The autoimmune responses in Treg cell-specific heterozygous Cdc42 knockout mice, CASIN-treated C57BL/6 mice, and control mice were assessed by H&E staining and ELISA. Antitumor T-cell immunity in Treg cell-specific heterozygous Cdc42 knockout mice, CASIN-treated C57BL/6 mice, humanized NSGS mice, and control mice was assessed by challenging the mice with MC38 mouse colon cancer cells, KPC mouse pancreatic cancer cells, or HCT116 human colon cancer cells.

Results Treg cell-specific heterozygous deletion or pharmacological targeting of Cdc42 with CASIN does not affect Treg cell numbers but induces Treg cell instability, leading to antitumor T-cell immunity without detectable autoimmune reactions. Cdc42 targeting causes an additive effect on immune checkpoint inhibitor anti-programmed cell death protein-1 antibody-induced T-cell response against mouse and human tumors. Mechanistically, Cdc42 targeting induces Treg cell instability and unleashes antitumor T-cell immunity through carbonic anhydrase I-mediated pH changes.

Conclusions Rational targeting of Cdc42 in Treg cells holds therapeutic promises in cancer immunotherapy.

INTRODUCTION

CD4⁺ and CD8⁺ effector T lymphocytes have the potential to inhibit tumor cells. However,

WHAT IS ALREADY KNOWN ON THIS TOPIC

⇒ The current immunotherapies only benefit a small proportion of patients with cancer. Targeting regulatory T (Treg) cells is viewed as an alternative cancer immunotherapy strategy, however, systemic depletion of Treg cells may cause autoimmunity. It has recently been suggested that cancer may be treated by induction of Treg cell instability.

WHAT THIS STUDY ADDS

⇒ Genetic or pharmacologic targeting of Cdc42 GTPase destabilizes Treg cells without affecting their homeostasis and triggers antitumor T-cell immunity without causing autoimmunity.

HOW THIS STUDY MIGHT AFFECT RESEARCH, PRACTICE OR POLICY

⇒ Rational targeting of Cdc42 in Treg cells holds therapeutic promises in cancer immunotherapy.

tumor cells can evade immune surveillance partly by engaging immune checkpoint proteins (eg, programmed cell death protein-1 (PD-1), cytotoxic T-lymphocyte-associated protein 4 (CTLA-4)) on effector T cells to cause their exhaustion.¹ Several immune checkpoint inhibitors (ICIs) (eg, anti-PD-1) have been approved by the Food and Drug Administration (FDA) for the treatment of a number of cancer types.² However, these ICIs are only efficacious in a small proportion of patients with cancer,³ necessitating improved cancer immunotherapies.

CD4⁺Foxp3⁺ regulatory T (Treg) cells are important for maintaining immune tolerance, primarily by inhibiting effector T cells.⁴ Consequently, defects in Treg cell homeostasis or their suppressive function can lead to excessive effector T-cell responses and autoimmunity.^{5,6} In the tumor microenvironment (TME), Treg cells contribute to tumor immune evasion.^{7,8} Depletion of Treg cells may thus benefit patients with cancer.⁹ However, systemic removal of Treg cells

likely causes autoimmune diseases.⁹ It has recently been suggested that cancer may be treated by induction of Treg cell instability that in general is reflected by loss of stable expression of Foxp3, the signature transcription factor and an important functional marker of Treg cells, effector T-cell reprogramming, and/or impairment of Treg cell function.^{10–13} The mechanisms underlying Treg cell instability remain poorly defined, understanding of which may provide novel biological targets for cancer immunotherapy.

Cdc42 is a Rho family GTPase that regulates a variety of cellular events including cell proliferation, survival, actin cytoskeletal organization, and migration.¹⁴ We have recently reported that Treg cell-specific homozygous gene deletion of *Cdc42* decreases Treg cell numbers, induces Treg cell instability, and causes early, fatal inflammatory diseases.¹⁵ This suggests that Cdc42 is important for maintenance of Treg cell homeostasis and stability and for controlling autoimmunity. Here we report that Treg cell-specific heterozygous gene deletion of *Cdc42* also induces Treg cell instability but does not reduce Treg cell number nor does it cause autoimmunity. Importantly, heterozygous deletion of *Cdc42* activates antitumor T-cell immunity. Mechanistically, heterozygous deletion of *Cdc42* induces Treg cell instability and unleashes antitumor T-cell immunity through upregulation of carbonic anhydrase I (CAI) that functions to modulate cellular pH by catalyzing the hydration of CO₂ to HCO₃[−] and H⁺.¹⁶ A Cdc42 inhibitor, CASIN,¹⁷ mimics heterozygous deletion of *Cdc42* in inducing Treg cell instability and causes antitumor T-cell immunity, without incurring autoimmune responses. Additionally, CASIN synergizes with anti-PD-1 in triggering antitumor T-cell immunity. Our findings indicate that pharmacological titration of Cdc42 to induce Treg cell instability without altering their homeostasis may be useful for immunotherapy modulations without causing autoimmunity.

METHODS

Tumor growth studies and treatments

Unless otherwise noted, 8×10⁵ MC38 or KPC tumor cells were injected subcutaneously in 100μL phosphate-buffered saline (PBS) into one of the flanks of the indicated mice. Two million HCT116 cells were injected subcutaneously in 100μL PBS into one flank of NSGS mice 15 weeks after the mice were transplanted with CD34⁺ hematopoietic stem cells.¹⁸ Wherever possible, animals were randomized into treatment groups. Tumor volumes were measured every day after the tumor became visible and calculated as V=(length×width²×0.50). All the mice were euthanized when tumor volume of control mice reached about 2cm³ (unless otherwise noted) and tumors were harvested.

CASIN (Cayman Chemical, 17694) in 60% PBS and 40% β-cyclodextrin (Cayman Chemical, 23387) was injected intraperitoneally (i.p.) at 30mg/kg two times per day for 7 days and then 40mg/kg one time per day

until the end of the experiments. For prophylactic treatment, CASIN injection was started at the same time as tumor cell injection. For therapeutic treatment, CASIN injection was started at around day 10 when tumors became visible. Carbonic anhydrase (CA) inhibitor acetazolamide (Sigma-Aldrich, A6011) in 90% PBS, 5% Tween-20 and 5% polyethylene glycol was injected i.p. at 40mg/kg one time per day. Wiskott-Aldrich syndrome protein (WASP) inhibitor wiskostatin (Cayman Chemical, 15047) in 97.5% PBS and 2.5% dimethyl sulfoxide was injected i.p. at 60mg/kg one time per day. GATA binding protein 3 (GATA3) inhibitor pyrrothiogatain (Santa Cruz, sc-352288A) in 90% PBS, 5% Tween-20 and 5% polyethylene glycol was injected i.p. at 60mg/kg one time per day. For T-cell depletion experiments, anti-CD4 (150μg/mouse) (Bio X Cell, BE0003-3, Clone ID: YTS 177, RRID:AB_1107642), anti-CD8 (150μg/mouse) (Bio X Cell, BE0118, Clone ID: HB-129, RRID: AB_10949065), or rat IgG2a isotype control (150μg/mouse) (Bio X Cell, BE0090, Clone ID: LTF-2, RRID:AB_1107780) were injected i.p. every other day for four injections and then two times a week until the end of the experiments. Injection of acetazolamide, wiskostatin, pyrrothiogatain, or anti-CD4/CD8 was started at the same time as tumor cell injection. For Treg cell depletion experiment, anti-CD25 (500μg/mouse) (Bio X Cell, BE0012, Clone ID: PC61.5.3, RRID: AB_1107619) or rat IgG1 isotype control (500μg/mouse) (Bio X Cell, BE0088, Clone ID: HRPN, RRID: AB_1107775) was injected i.p. 1 day before tumor cell injection.¹⁹ For experiments involving ICIs, anti-PD-1 (150μg/mouse) (Bio X Cell, BE0146, Clone ID: RMP1-14, RRID: AB_10949053) was injected every other day for a total of five injections starting on tumor onset. The order of treatments was not controlled.

Adoptive cell transfer studies

Splenic Treg cells were obtained by magnetic-activated cell sorting of CD4⁺ T cells (Miltenyi, 130-117-043) followed by fluorescence-activated cell sorting (FACS) of CD4⁺YFP⁺ Treg cells to >99% purity. Splenic T cells were isolated from congenic BoyJ mice by a pan T-cell isolation kit (Miltenyi, 130-095-130) followed by Treg cell depletion with CD25 MicroBead Kit (Miltenyi, 130-091-072). The sorted Treg cells (2–3×10⁵ per mouse) with or without congenic T cells (6×10⁵ per mouse) were transferred i.p. into *Rag1*^{−/−} mice 1 day before or 9 days after MC38 cell injection into the recipient mice.

Flow cytometry

Spleens were mashed with a syringe plunger and passed through 40μm cell strainer, followed by treatment with red blood cell lysis buffer (BD Biosciences, 555899). Tumors were minced into small fragments and treated with 1.5mg/mL collagenase IV (Sigma, C5138) for 30min at 37°C under agitation. The digested tumor tissue was then filtered through a 70μm cell strainer and centrifuged at 1500rpm at 4°C for 5 min. The pellets were dissolved in 8mL of 40% percoll and slowly layered over

5 mL of 80% percoll in a 15 mL falcon tube. The falcon tube was then centrifuged at 2000 rpm at 4°C for 20 min, stopping without brakes. Cells at the interface between 40% percoll and 80% percoll were carefully removed and washed twice with complete Roswell Park Memorial Institute (RPMI) T-cell medium. The cells from spleens and tumors were restimulated with phorbol 12-myristate 13-acetate (PMA) and ionomycin for 5 hours in the presence of GolgiPlug for the last 4 hours, and then subjected to antibody staining (see online supplemental materials and methods for the list of antibodies). The stained cells were analyzed by BD LSRII, FACSCanto, or LSRFortessa flow cytometers. Data were analyzed with BD FACSDiva.

In certain experiments, Treg cells isolated by flow cytometry sorting of CD4⁺YFP⁺ cells to >99% purity were expanded with Treg cell expansion kit (Miltenyi, 130-095-925) for 3 days, in the presence or absence of 47.6 mM NaHCO₃ (to make culture medium of pH 7.60), 3 μM acetazolamide, 50 μM pyrrothiogatain, or the indicated concentrations of wiskostatin or CASIN. The cells were then subjected to the indicated analysis. For cytokine detection, the cells were restimulated with PMA and ionomycin along with GolgiPlug followed by flow cytometry analysis. For lentiviral shRNA-mediated knockdown, scrambled shRNA, CAI shRNA, and GATA3 shRNA lentiviral supernatants were produced by transfection of 293T cells with packaging lentiviral plasmids and either scrambled shRNA (Origene, TR30021), CAI shRNA (Origene, TL510087) or GATA3 shRNA (Origene, TL513036) lentiviral vectors followed by concentrating with Lenti-X concentrator (Takara, 631231). The viral supernatants were transduced into Treg cells that were expanded for 1 day before the transduction, by centrifugation at 1000 g at 32°C for 90 min. The transduced Treg cells were further expanded for another 2 days and subjected to the indicated analysis.

For 5-bromo-29-deoxyuridine (BrdU) incorporation assay, mice were injected i.p. with 500 mg BrdU. Two hours after injection, splenocytes were isolated and immunolabeled with anti-CD4 and anti-Foxp3 antibodies and BrdU incorporation was analyzed by a BrdU Flow kit per the manufacturer's protocol (BD Pharmingen, 552598).¹⁵

For cell apoptosis assay, freshly isolated splenocytes were immunolabeled with anti-CD4 and anti-Foxp3 antibodies and cell apoptosis was analyzed by anti-active caspase 3 antibody (BD Pharmingen, 559341, Clone ID: C92-605, RRID:AB_397234) staining followed by flow cytometry.

Autoantibody detection

Serum was isolated from blood using serum separator tubes. Anti-dsDNA and ANA in serum were detected by ELISA using the corresponding ELISA Kits (Alpha Diagnostic International, 5120-1 and 5210, respectively), according to the manufacturer's protocol.

Bisulfite pyrosequencing of methylation of Foxp3 enhancer

A total of 200 ng genomic DNA was subjected to sodium bisulfite treatment and purified using the EZ DNA

Methylation-Gold Kit (Zymo research, D5007) according to the manufacturer's specifications. Two rounds of standard polymerase chain reaction (PCR) amplification reaction were performed to amplify targeted gene fragment at an annealing temperature of 50°C before being subjected to pyrosequencing. The generated pyrograms were automatically analyzed using PyroMark analysis software (Qiagen). The pyrosequencing assay was validated using SssI-treated human genomic DNA as a 100% methylation control and human genomic DNA amplified by GenomePlex Complete Whole Genome Amplification kit (Sigma-Aldrich, WGA2-50RXN) as 0% methylation control.¹⁵ The primers used for bisulfite pyrosequencing are listed in online supplemental materials and methods.

Histopathological analysis

Tissues were sectioned, fixed in 4% formaldehyde solution, embedded in paraffin, and stained with H&E. The sections were analyzed by light microscopy from Fisher Scientific Moticam at 20× magnification at room temperature. The images were acquired by using the software Motic Images Plus V.2.0.¹⁵

Quantitative real-time reverse transcription (RT)-PCR analysis

Total RNA was extracted with the RNeasy mini kit from Qiagen. Isolated RNA was converted to complementary DNA (cDNA) by using High-Capacity cDNA Reverse Transcription Kit (Applied Biosystems, 4368814). Real-time RT-PCR was performed with Platinum SYBR Green qPCR SuperMix-UDG with ROX (Invitrogen, 11-744-500) and measured on StepOnePlus Real-Time PCR System (Applied Biosystems, 4376600). Data were normalized to 18S rRNA. The primers used are listed in online supplemental materials and methods.

Chromatin immunoprecipitation-quantitative real-time PCR

Treg cells were fixed with 1% formaldehyde at room temperature for 10 min. Formaldehyde was quenched by addition of 0.125 M glycine and incubation for another 5 min. The cells were lysed in 1 mL buffer 1 (50 mM HEPES (pH 7.5), 140 mM NaCl, 1 mM EDTA, 0.5% NP-40, 0.25% Triton X-100, and 10% glycerol) supplemented with protease inhibitor cocktail (Roche, 36363600) for 10 min. Nuclei were collected and resuspended in 1 mL buffer 2 (10 mM Tris (pH 8.0), 200 mM NaCl, 0.5 mM EGTA and 1 mM EDTA), and incubated at 4°C for 10 min. Pelleted nuclei were resuspended and sonicated for 10 min in 1 mL sonication buffer (100 mM NaCl, 50 mM Tris (pH 8), 5 mM EDTA pH 8, and 0.5% SDS) in a Covaris sonicator. After removal of an input control (whole cell lysate), chromatin was incubated with anti-GATA3 antibody (Invitrogen, MA1-028, Clone ID: 1A12-1D9, RRID:AB_2536713) or normal mouse IgG (Santa Cruz, sc-2025, RRID:AB_737182) at 4°C overnight, and pre-blocked Dynabeads Protein G for Immunoprecipitation (Thermo Fisher Scientific, 10003D) were added to the samples. After incubation at 4°C for 2 hours, the beads were washed with wash buffer 1 (150 mM NaCl, 20 mM Tris

(pH 8), 5 mM EDTA (pH 8), 1% Triton X-100 and 0.2% SDS), Buffer 2 (0.1% deoxycholic acid, 1 mM EDTA (pH 8), 50 mM HEPES (pH 7.5), 1% Triton X-100, 500 mM NaCl), LiCl buffer (10 mM Tris (pH 8), 0.5% deoxycholic acid, 1 mM EDTA (pH 8), 250 mM LiCl, 0.5% NP-40), and Tris-EDTA (TE). DNA was eluted in elution buffer (0.1% SDS) and crosslinking was reversed by incubation at 65°C for 10 hours.²⁰ After RNase A and proteinase K treatment, the precipitated chromatin DNA was purified by using a PCR purification kit (Qiagen, 28104) and then subjected to quantitative real-time PCR with the TaqMan Universal PCR Master Mix (Thermo Fisher Scientific, 4304437). Primers targeting the *Car1* locus containing GATA3 binding site are: Forward 5' GTTGTCAGTTGCCTGG-CATC 3'; Reverse: 5' GACAGTGGTAGTGGCTGCAC 3'.

Statistical analysis

Statistical analysis was carried out using Microsoft Excel 2013. Tumor growth and body weight loss in dextran sulfate sodium (DSS)-induced mouse model of colitis were analyzed by two-way analysis of variance. The rest of the statistics were performed with Mann-Whitney test. Data were expressed as mean±SD. P value<0.05 was considered significant.

RESULTS

Heterozygous deletion of *Cdc42* induces Treg cell instability but does not cause autoimmunity

By crossing *Cdc42*^{Flox/Flox} mice with *Foxp3*^{YFP-Cre} mice, we generated *Cdc42*^{Flox/+}*Foxp3*^{YFP-Cre} mice that harbor heterozygous knockout of *Cdc42* specifically in Treg cells. We found that heterozygous knockout of *Cdc42* did not affect Treg cell homeostasis (figure 1A), proliferation (figure 1B), and survival (figure 1C). A variety of Treg cell functional markers such as PD-1, CTLA-4, ICOS, GITR, CD39, and CD73 also remained unchanged (figure 1D and online supplemental figure 1A). *Cdc42*^{Flox/+}*Foxp3*^{YFP-Cre} mice had no visible inflammatory disorders. H&E staining showed no inflammatory cell infiltration into the colon, liver, lung, and kidney of *Cdc42*^{Flox/+}*Foxp3*^{YFP-Cre} mice (figure 1E). However, *Cdc42*^{Flox/+}*Foxp3*^{YFP-Cre} Treg cells showed reduced expression of *Foxp3* (figure 1F) and increased methylation in conserved non-coding sequence 2 (CNS2) of the *Foxp3* locus (figure 1G), a CpG-rich *Foxp3* intronic cis-element whose hypomethylation is important for stable *Foxp3* expression.¹³ The increased methylation in CNS2 of the *Foxp3* locus was associated with increased expression of *DNA methyltransferase 3A* (*DNMT3a*) but not alteration in *DNA demethylases TET1/2/3* (online supplemental figure 1B). *Cdc42*^{Flox/+}*Foxp3*^{YFP-Cre} Treg cells underwent effector T-cell reprogramming, as evidenced by increased expression of interleukin (IL)-4, a signature cytokine of CD4⁺ T helper 2 (Th2) cells, and interferon (IFN)-γ, a signature cytokine of CD4⁺ Th1 cells, but not IL-17, a signature cytokine of CD4⁺ Th17 cells (figure 1H and online supplemental figure 2A). Although IFN-γ-expressing CD8⁺ effector T cells were not altered (figure 1I

and online supplemental figure 2B), IL-4-expressing and IFN-γ-expressing CD4⁺ effector T cells (CD4⁺*Foxp3*[−]) were increased in *Cdc42*^{Flox/+}*Foxp3*^{YFP-Cre} mice (figure 1J and online supplemental figure 2A). Likewise, heterozygous deletion of *Cdc42* in Treg cells did not affect CD62L⁺CD44[−] naïve T cells, CD62L⁺CD44⁺ central memory T cells and CD62L[−]CD44⁺ effector memory T cells in CD8⁺ T-cell compartment (figure 1K) but increased memory T cells at the expense of naïve T cells in CD4⁺ T-cell compartment (figure 1L). The increased CD4⁺ memory T cells may reflect the increased IL-4-producing and IFN-γ-producing CD4⁺ T cells that would have resulted from a conversion of unstable Treg cells to effector T cells. In support, ex vivo culture of Treg cells found that heterozygous loss of *Cdc42* caused more Treg cell conversion to CD4⁺*Foxp3*[−] ex-Treg cells (figure 1M). To determine whether the same occurs in vivo, we took advantage of *Foxp3*^{Cre}*GFP-Cre-ERT2*[−]*Rosa26*^{eYFP} mice. In *Foxp3*^{Cre}*GFP-Cre-ERT2*[−]*Rosa26*^{eYFP} mice, treatment with tamoxifen induces the expression of Cre and GFP in *Foxp3*⁺ cells. Cre expression causes excision of floxed stop codon in the *Rosa26* locus, leading to YFP expression. Thus, Treg cells from *Foxp3*^{Cre}*GFP-Cre-ERT2*[−]*Rosa26*^{eYFP} mice are marked by both GFP and YFP. When Treg cells convert to CD4⁺*Foxp3*[−] ex-Treg cells, their GFP is lost but YFP is retained, because the *Rosa26* locus is ubiquitously expressed.²¹ We crossed *Foxp3*^{Cre}*GFP-Cre-ERT2*[−]*Rosa26*^{eYFP} mice with *Cdc42*^{Flox/Flox} mice and found that the resultant *Cdc42*^{Flox/+}*Foxp3*^{Cre}*GFP-Cre-ERT2*[−]*Rosa26*^{eYFP} mice contained more CD4⁺GFP[−]YFP⁺ ex-Treg cells, compared with *Cdc42*^{+/+}*Foxp3*^{Cre}*GFP-Cre-ERT2*[−]*Rosa26*^{eYFP} mice (figure 1N). Together, these results indicate that heterozygous loss of *Cdc42* primes Treg cell instability without invoking autoimmune responses.

Treg cell-specific heterozygous deletion of *Cdc42* inhibits tumor growth

To determine whether *Cdc42*^{Flox/+}*Foxp3*^{YFP-Cre} Treg cells can be harnessed for tumor control, we inoculated *Cdc42*^{Flox/+}*Foxp3*^{YFP-Cre} and control *Cdc42*^{+/+}*Foxp3*^{YFP-Cre} mice with MC38 mouse colon cancer cells. We found that tumor growth (measured by tumor volume) was drastically suppressed in *Cdc42*^{Flox/+}*Foxp3*^{YFP-Cre} mice (figure 2A). Although *Cdc42*^{Flox/+}*Foxp3*^{YFP-Cre} mice did not show a change in the ratio of tumor-infiltrating effector T cells versus Treg cells (figure 2B), these mice had increased tumor-infiltrating IFN-γ⁺ Treg cells (figure 2C and online supplemental figure 3A) and effector T cells (figure 2D and E and online supplemental figure 3B, C). A modest increase in IFN-γ-producing Treg cells and CD4⁺ effector T cells and a marked increase in IFN-γ-producing CD8⁺ effector T cells were also observed in the spleen of tumor-bearing *Cdc42*^{Flox/+}*Foxp3*^{YFP-Cre} mice (online supplemental figure 3D–F), indicating that *Cdc42* heterozygosity generates a global immuno-effect in tumor-bearing mice. Nonetheless, IFN-γ⁺ cells seemed to be less in the spleen than that in tumor (online supplemental figure 3D–F compared with figure 2C–E), suggesting that IFN-γ⁺ cells unproportionally migrated from tumor/tumor draining

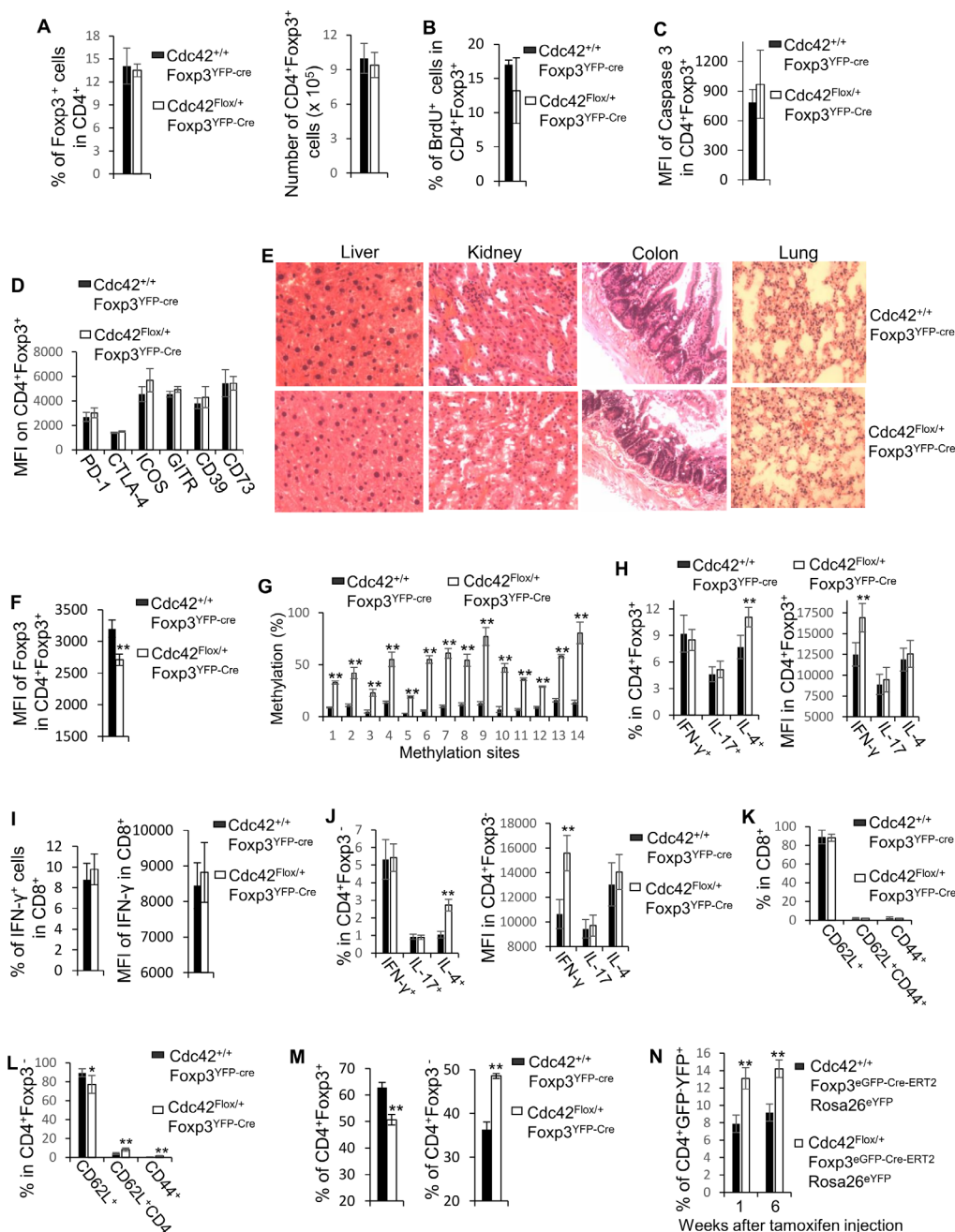


Figure 1 Heterozygous loss of *Cdc42* in Treg cells induces Treg cell instability and increases CD4⁺ effector T cells but does not result in autoimmunity. (A–M) The spleen from wild type (*Cdc42*^{+/+}*Foxp3*^{YFP-Cre}) and *Cdc42* heterozygous knockout (*Cdc42*^{Flox/+}*Foxp3*^{YFP-Cre}) mice was subjected to flow cytometry analysis of the percentages and number of Treg cells (A), Treg cell proliferation (BrdU incorporation) (B), Treg cell apoptosis (expression of cleaved caspase 3) (C), Treg cell functional markers (D), the expression of Foxp3 (MFI) in Treg cells (F), the expression (percentages and MFI) of IFN-γ, IL-17 and/or IL-4 in Treg cells (H), CD8⁺ T cells (I) and CD4⁺ T cells (J), and the percentages of naïve (CD62L⁺CD44⁺), central memory (CD62L⁺CD44⁺) and effector memory (CD62L⁺CD44⁺) T cells in CD8⁺ (K) and CD4⁺ (L) T-cell compartments. Of note, MFI of IFN-γ, IL-17 and IL-4 was analyzed in IFN-γ⁺, IL-17⁺ and IL-4⁺ cells, respectively. Splenic Treg cells from the mice were examined for the methylation status of 14 methylation sites of the Foxp3 conserved non-coding sequence 2 by bisulfite pyrosequencing (G) or cultured for 3 days followed by flow cytometry analysis of induction of ex-Treg cells (CD4⁺Foxp3⁺) (M). The liver, kidney, colon, and lung from the mice were subjected to H&E staining (E). (N) *Cdc42*^{Flox/+}*Foxp3*^{eGFP-Cre-ERT2}*Rosa26*^{eYFP} and *Cdc42*^{+/+}*Foxp3*^{eGFP-Cre-ERT2}*Rosa26*^{eYFP} mice were treated (intraperitoneally) with 2 mg of tamoxifen daily for five consecutive days. One week and 6 weeks after the last tamoxifen injection, the spleen was analyzed for CD4⁺GFP⁺YFP⁺ ex-Treg cells by flow cytometry. (A–D, F, and H–L) Error bars indicate SD of 5–8 mice. Data are representative of three independent experiments. (N) Error bars indicate SD of five mice. Data are representative of two independent experiments. (G and M) Error bars indicate SD of triplicates. Data are from one experiment with four mice pooled. (G) Data are expressed as percentage of methylation which indicates per cent cells with a particular methylation site methylated. **p*<0.05; ***p*<0.01. BrdU, bromo-29-deoxyuridine; IFN, interferon; IL, interleukin; MFI, mean fluorescence intensity; Treg, regulatory T cells.

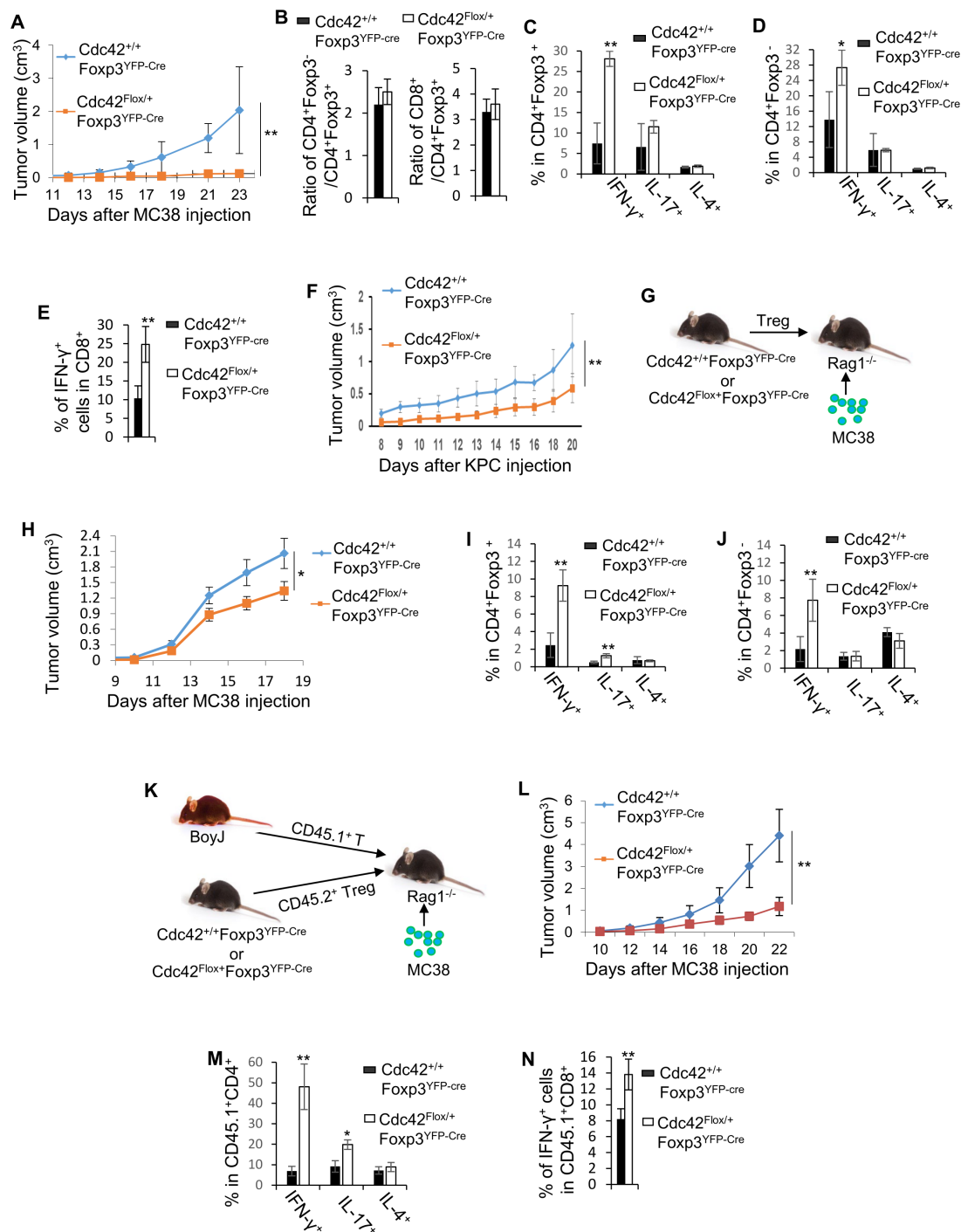


Figure 2 Heterozygous loss of *Cdc42* in Treg cells inhibits tumor growth by promoting Treg cell instability. (A–F) MC38 colon cancer cells (A–E) or KPC pancreatic cancer cells (F) were inoculated into *Cdc42*^{+/+}*Foxp3*^{YFP-Cre} and *Cdc42*^{Flox/+}*Foxp3*^{YFP-Cre} mice. Tumor growth (volume) was recorded (A, F). Tumor was dissected and subjected to flow cytometry analysis of the percentages of CD4⁺Foxp3⁺ Treg cells and CD4⁺Foxp3⁺ T cells among total CD4⁺ T cells, and the percentages of total CD4⁺Foxp3⁺ Treg cells and CD8⁺ T cells from singlet cells. The ratio of CD4⁺Foxp3⁺ T cells versus CD4⁺Foxp3⁺ Treg cells and the ratio of total CD4⁺ T cells versus total CD4⁺Foxp3⁺ Treg cells were calculated (B). IFN- γ ⁺, IL-17⁺ and/or IL-4⁺ cells in tumor-infiltrating CD4⁺Foxp3⁺ Treg cells (C), CD4⁺Foxp3⁺ T cells (D) and CD8⁺ T cells (E) were also analyzed by flow cytometry. (G–J) *Cdc42*^{+/+}*Foxp3*^{YFP-Cre} or *Cdc42*^{Flox/+}*Foxp3*^{YFP-Cre} Treg cells were adoptively transferred into Rag1^{-/-} mice. One day later, the recipient mice were inoculated with MC38 cells (G). Tumor volume was recorded (H). The percentages of IFN- γ ⁺, IL-17⁺ and/or IL-4⁺ cells in tumor-infiltrating Treg cells (CD4⁺Foxp3⁺) (I) and CD4⁺ effector T cells (CD4⁺Foxp3⁺) (J) were analyzed by flow cytometry. (K–N) *Cdc42*^{+/+}*Foxp3*^{YFP-Cre} or *Cdc42*^{Flox/+}*Foxp3*^{YFP-Cre} Treg cells were adoptively co-transferred with congenic T cells into Rag1^{-/-} mice. One day later, the recipient mice were inoculated with MC38 cells (K). Tumor volume was recorded (L). The percentages of IFN- γ ⁺, IL-17⁺ and/or IL-4⁺ cells in tumor-infiltrating congenic CD4⁺ (M) and CD8⁺ (N) effector T cells were analyzed by flow cytometry. Error bars indicate SD of 5–6 mice. Data are representative of two independent experiments. **p*<0.05; ***p*<0.01. IFN, interferon; IL, interleukin; Treg, regulatory T cells.

lymph nodes to the spleen. Furthermore, heterozygous loss of *Cdc42* in Treg cells inhibited tumor growth of KPC pancreatic cancer cells (figure 2F). Together, these results suggest that unstable *Cdc42^{Flox/+}Foxp3^{YFP-Cre}* Treg cells trigger T-cell immunity against tumor growth.

The tumor suppression in *Cdc42^{Flox/+}Foxp3^{YFP-Cre}* mice may be mediated by the increased CD4⁺ effector T cells that are converted from unstable Treg cells. To test this possibility, we transferred *Cdc42^{Flox/+}Foxp3^{YFP-Cre}* and *Cdc42^{+/-}Foxp3^{YFP-Cre}* Treg cells into immunodeficient *Rag1^{-/-}* mice followed by MC38 tumor cell inoculation (figure 2G). We found that tumor growth was modestly but significantly inhibited in the mice receiving *Cdc42^{Flox/+}Foxp3^{YFP-Cre}* Treg cells (figure 2H). Tumors in the mice receiving *Cdc42^{Flox/+}Foxp3^{YFP-Cre}* Treg cells showed an increase in unstable Treg cells (figure 2I) and in CD4⁺ effector T cells (figure 2J). As only Treg cells were transferred, the increased CD4⁺ effector T cells were presumably ex-Treg cells converted from unstable *Cdc42^{Flox/+}Foxp3^{YFP-Cre}* Treg cells, similar to that on ex vivo culture (figure 1M) and in Treg lineage tracing mice (figure 1N). It is conceivable that these ex-Treg cells contributed to the tumor suppression. However, we cannot rule out that effector T-cell activities (eg, IFN- γ production) in Treg cells may have also played a role in the tumor suppression. Taken together, our data demonstrate that the instability of *Cdc42^{Flox/+}Foxp3^{YFP-Cre}* Treg cells contributes to the tumor suppression in *Cdc42^{Flox/+}Foxp3^{YFP-Cre}* mice.

The tumor suppression in *Cdc42^{Flox/+}Foxp3^{YFP-Cre}* mice may also be mediated by dampened suppressive function of unstable Treg cells.^{11,12} In this context, the increased CD4⁺ effector T cells in *Cdc42^{Flox/+}Foxp3^{YFP-Cre}* mice may not only result from unstable Treg cell conversion to effector T cells but also compromised function of *Cdc42^{Flox/+}Foxp3^{YFP-Cre}* Treg cells, which is supported by the increased CD8⁺ effector T cells in tumor-bearing *Cdc42^{Flox/+}Foxp3^{YFP-Cre}* mice. To test this, we co-transferred *Cdc42^{Flox/+}Foxp3^{YFP-Cre}* or *Cdc42^{+/-}Foxp3^{YFP-Cre}* Treg cells with congenically marked (CD45.1⁺) effector T cells into *Rag1^{-/-}* mice followed by tumor cell inoculation (figure 2K). As expected, tumor growth in the mice receiving *Cdc42^{Flox/+}Foxp3^{YFP-Cre}* Treg cells and effector T cells was inhibited (figure 2L). The mice contained increased tumor-infiltrating CD45.1⁺ effector T cells (figure 2M,N), suggesting that *Cdc42^{Flox/+}Foxp3^{YFP-Cre}* Treg cells were indeed impaired in their suppressive function. In this setting, the co-transfer of *Cdc42^{Flox/+}Foxp3^{YFP-Cre}* Treg cells with effector T cells appeared to diminish tumor growth to a greater extent than the transfer of *Cdc42^{Flox/+}Foxp3^{YFP-Cre}* Treg cells only (figure 2L, compared with figure 2H), suggesting that the dampened suppressive function of *Cdc42^{Flox/+}Foxp3^{YFP-Cre}* Treg cells also contributes to the tumor suppression in *Cdc42^{Flox/+}Foxp3^{YFP-Cre}* mice.

Of note, unstable Treg cells (online supplemental figure 4A, B) and/or the resultant effector T cells (online supplemental figure 4C,D) in 12–18 months old *Cdc42^{Flox/+}Foxp3^{YFP-Cre}* mice did not cause spontaneous systemic inflammatory disorders (online supplemental figure 4E),

similar to that in 6–8 weeks old *Cdc42^{Flox/+}Foxp3^{YFP-Cre}* mice (figure 1) but distinct from that in aged *CNS2^{-/-}* mice that show spontaneous lymphoproliferative disease.²² We speculate that the instability phenotypes of *Cdc42^{Flox/+}Foxp3^{YFP-Cre}* Treg cells may be milder than that of aged *CNS2^{-/-}* Treg cells. As that in 6–8 weeks old *Cdc42^{Flox/+}Foxp3^{YFP-Cre}* mice (figure 2), *Cdc42^{Flox/+}Foxp3^{YFP-Cre}* Treg cells in 12–18 months old *Cdc42^{Flox/+}Foxp3^{YFP-Cre}* mice were able to cause tumor suppression attributable to instability of tumor-infiltrating Treg cells (online supplemental figure 4F–I).

Treg cell-specific heterozygous deletion of *Cdc42* induces Treg cell instability and elicits antitumor T-cell immunity through a WASP-GATA3-CAI signaling node

To determine the mechanism of heterozygous *Cdc42* loss-induced Treg cell instability, we carried out global gene expression profiling of *Cdc42^{Flox/+}Foxp3^{YFP-Cre}* Treg and *Cdc42^{+/-}Foxp3^{YFP-Cre}* Treg cells, by RNA sequencing. We found that 319 genes were upregulated (>1.2-fold) and 140 genes were downregulated (>1.2-fold) in *Cdc42^{Flox/+}Foxp3^{YFP-Cre}* Treg cells (online supplemental table 1). Kyoto Encyclopedia of Genes and Genomes (KEGG) pathway analysis found that cytokine–cytokine receptor interaction pathway was upregulated (FDR <0.25) (online supplemental table 2) and ribosome pathway was downregulated (FDR <0.25) (online supplemental Table 3) in *Cdc42^{Flox/+}Foxp3^{YFP-Cre}* Treg cells. Among the upregulated genes, *Car1* that encodes CAI was of particular interest, since it is the second most upregulated gene in *Cdc42^{Flox/+}Foxp3^{YFP-Cre}* Treg cells (online supplemental table 1 and figure 5A) and the most upregulated gene in *Cdc42^{Flox/+}Foxp3^{YFP-Cre}* Treg cells (online supplemental table 4 and figure 5B). The expression levels of CAI messenger RNA (mRNA) were 369-fold in *Cdc42^{Flox/+}Foxp3^{YFP-Cre}* Treg cells and 7828-fold in *Cdc42^{Flox/Flox}Foxp3^{YFP-Cre}* Treg cells more than that in *Cdc42^{+/-}Foxp3^{YFP-Cre}* Treg cells (online supplemental tables 1 and 4). We confirmed the upregulation of CAI mRNA and CAI protein in *Cdc42^{Flox/+}Foxp3^{YFP-Cre}* Treg cells (figure 3A and online supplemental figure 6A). CAI functions to modulate cellular pH by catalyzing the hydration of CO₂ to HCO₃⁻ and H⁺.¹⁶ CAI is expressed in the cytoplasm.¹⁶ We hypothesized that overexpression of CAI in *Cdc42^{Flox/+}Foxp3^{YFP-Cre}* Treg cells generated excessive HCO₃⁻ and H⁺, leading to HCO₃⁻ transportation to extracellular space and thus extracellular alkalization that caused Treg cell instability. To test this, we measured the medium pH of *Cdc42^{Flox/+}Foxp3^{YFP-Cre}* and *Cdc42^{+/-}Foxp3^{YFP-Cre}* Treg cell culture. We found that while the pH of *Cdc42^{+/-}Foxp3^{YFP-Cre}* Treg cell culture was maintained at 7.40, the pH of *Cdc42^{Flox/+}Foxp3^{YFP-Cre}* Treg cell culture was changed to 7.60 (figure 3B). Importantly, *Cdc42^{+/-}Foxp3^{YFP-Cre}* Treg cells became unstable on incubation with culture medium of pH 7.60 (figure 3C–E) or with conditional medium from *Cdc42^{Flox/+}Foxp3^{YFP-Cre}* Treg cell culture (figure 3F–H). The extracellular alkalization and instability of *Cdc42^{Flox/+}Foxp3^{YFP-Cre}* Treg cells were rescued by treatment with a CA inhibitor, acetazolamide (figure 3I–K), and by CAI knockdown (figure 3L–O).

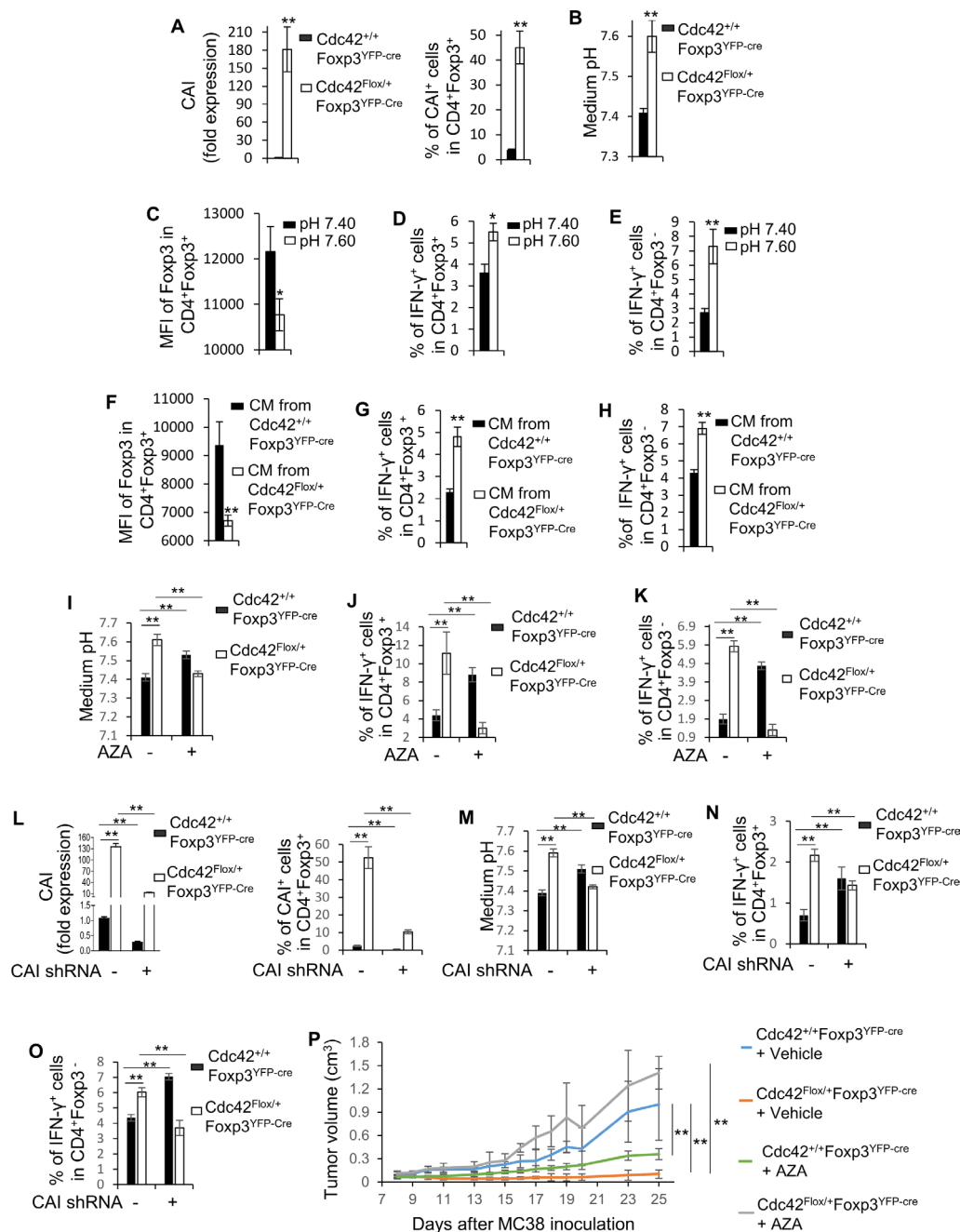


Figure 3 Heterozygous loss of *Cdc42* induces Treg cell instability and inhibits tumor growth through upregulation of CAI. (A, B) Splenic Treg cells from *Cdc42*^{+/+}*Foxp3*^{YFP-Cre} and *Cdc42*^{Flox/+}*Foxp3*^{YFP-Cre} mice were examined for the expression of CAI mRNA (left) and CAI protein (right) by quantitative real-time RT-PCR and flow cytometry, respectively (A), or cultured for 3 days followed by measurement of culture medium pH (B). (C–H) Splenic *Cdc42*^{+/+}*Foxp3*^{YFP-Cre} Treg cells were cultured for 3 days with medium of pH 7.40 or pH 7.60 (C–E) or with conditional medium from *Cdc42*^{+/+}*Foxp3*^{YFP-Cre} or *Cdc42*^{Flox/+}*Foxp3*^{YFP-Cre} Treg cell culture (F–H). The expression of Foxp3 (MFI) in Treg cells (C, F) and the percentages of IFN- γ ⁺ cells in Treg cells (D, G) and CD4⁺ effector T cells (ex-Treg) (E, H) were analyzed by flow cytometry. (I–K) Splenic *Cdc42*^{+/+}*Foxp3*^{YFP-Cre} and *Cdc42*^{Flox/+}*Foxp3*^{YFP-Cre} Treg cells were cultured for 3 days with AZA or vehicle. The medium pH was measured (I). The percentages of IFN- γ ⁺ cells in Treg cells (J) and CD4⁺ effector T cells (ex-Treg) (K) were analyzed by flow cytometry. (L–O) Splenic *Cdc42*^{+/+}*Foxp3*^{YFP-Cre} and *Cdc42*^{Flox/+}*Foxp3*^{YFP-Cre} Treg cells were transduced with CAI shRNA or scramble shRNA during 3 days' culture. The expression of CAI mRNA (left) and CAI protein (right) was detected by quantitative real-time RT-PCR and flow cytometry, respectively (L). The medium pH was measured (M). The percentages of IFN- γ ⁺ cells in Treg cells (N) and CD4⁺ effector T cells (ex-Treg) (O) were analyzed by flow cytometry. (P) *Cdc42*^{+/+}*Foxp3*^{YFP-Cre} and *Cdc42*^{Flox/+}*Foxp3*^{YFP-Cre} mice were inoculated with MC38 cells and treated with or without AZA at 40 mg/kg one time per day, starting at the same time as MC38 cell inoculation. Tumor volume was recorded. (A) Error bars indicate SD of four mice. (B–O) Error bars indicate SD of triplicates. Data are from five mice pooled. (P) Error bars indicate SD of four mice. Data are representative of two independent experiments. **p*<0.05; ***p*<0.01. AZA, acetazolamide; CAI, carbonic anhydrase I; IFN, interferon; MFI, mean fluorescence intensity; mRNA, messenger RNA; Treg, regulatory T cells; RT-PCR, reverse transcription polymerase chain reaction.

Thus, the instability of $Cdc42^{Fllox/+}Foxp3^{YFP-Cre}$ Treg cells is likely caused by CAI-mediated extracellular alkalization. Acetazolamide treatment of $Cdc42^{Fllox/+}Foxp3^{YFP-Cre}$ mice were able to restore tumor growth (figure 3P), correlating with reduced instability of tumor-infiltrating Treg cells and decreased tumor-infiltrating effector T cells (online supplemental Figure 6B-E). We conclude that heterozygous $Cdc42$ deletion induces Treg cell instability and revokes antitumor T-cell immunity through upregulation of CAI. Of note, inhibition of CAI in $Cdc42^{+/+}Foxp3^{YFP-Cre}$ Treg cells caused extracellular alkalization and Treg cell instability (figure 3I-K and L-O), similar to that caused by the upregulation of CAI in $Cdc42^{Fllox/+}Foxp3^{YFP-Cre}$ Treg cells (figure 3A, I-K and L-O). Furthermore, $Cdc42^{+/+}Foxp3^{YFP-Cre}$ mice treated with acetazolamide showed similar tumor suppression to $Cdc42^{Fllox/+}Foxp3^{YFP-Cre}$ mice (figure 3P). These data suggest that physiological levels of CAI are essential for Treg cell stability and Treg cell-mediated tumor growth. Given that only ~4% of $Cdc42^{+/+}Foxp3^{YFP-Cre}$ Treg cells expressed CAI (figure 3A), the drastic inhibition of tumor growth in acetazolamide-treated $Cdc42^{+/+}Foxp3^{YFP-Cre}$ mice suggests that even small proportion of CAI⁺ Treg cells could be important for maintaining overall Treg cell extracellular pH and their stability and that inhibition of CAI in tumor-infiltrating Treg cells may alter the TME pH, which may not only affect Treg cell stability but also other cells in the TME. It is conceivable that acetazolamide may directly affect effector T cells and/or MC38 tumor cells in tumor-bearing mice. Nonetheless, as effector T cells and MC38 tumor cells from $Cdc42^{Fllox/+}Foxp3^{YFP-Cre}$ mice presumably express CAI at comparable levels to that from $Cdc42^{+/+}Foxp3^{YFP-Cre}$ mice, any direct effect of acetazolamide on effector T cells and MC38 tumor cells is expected to affect tumor growth similarly in $Cdc42^{Fllox/+}Foxp3^{YFP-Cre}$ and $Cdc42^{+/+}Foxp3^{YFP-Cre}$ mice. Indeed, we did not detect a change in CAI expression in tumor-infiltrating effector T cells from $Cdc42^{Fllox/+}Foxp3^{YFP-Cre}$ mice (data not shown). In this context, the restoration of tumor growth in acetazolamide-treated $Cdc42^{Fllox/+}Foxp3^{YFP-Cre}$ mice and the inhibition of tumor growth in acetazolamide-treated $Cdc42^{+/+}Foxp3^{YFP-Cre}$ mice unlikely resulted from an off-Treg cell effect of acetazolamide but from differential expression of CAI in $Cdc42^{Fllox/+}Foxp3^{YFP-Cre}$ and $Cdc42^{+/+}Foxp3^{YFP-Cre}$ Treg cells.

To define the mechanism underlying heterozygous $Cdc42$ deletion-induced CAI upregulation in Treg cells, we analyzed transcription factor binding sites at the *Car1* locus. We found that the *Car1* locus contained the GATA3 binding motif WGATAA (figure 4A) that was reported in Treg cells.²³ Interestingly, GATA3 was upregulated and its binding to the *Car1* locus was enhanced in $Cdc42^{Fllox/+}Foxp3^{YFP-Cre}$ Treg cells (figure 4B,C). We attempted to genetically delete *GATA3* in $Cdc42^{Fllox/+}Foxp3^{YFP-Cre}$ Treg cells to determine whether loss of *GATA3* could reverse CAI expression. However, we could not obtain $Cdc42^{Fllox/+}GATA3^{Fllox/Fllox}Foxp3^{YFP-Cre}$ compound mice, possibly due to that heterozygous $Cdc42$ deletion aggravates Treg cell-specific homozygous *GATA3* deletion-induced inflammatory

disorders.²⁴ Nonetheless, inhibition of GATA3 in $Cdc42^{Fllox/+}Foxp3^{YFP-Cre}$ Treg cells by an inhibitor of GATA3 DNA binding activity, pyrrothiogatain,²⁵ or GATA3 shRNA (figure 4G) significantly suppressed the increased CAI expression (figure 4D and H) and reduced $Cdc42^{Fllox/+}Foxp3^{YFP-Cre}$ Treg cell instability (figure 4E,F and I,J). This suggests that the increased GATA3 expression and its binding to the *Car1* locus contribute to the increased CAI expression and instability of $Cdc42^{Fllox/+}Foxp3^{YFP-Cre}$ Treg cells. Importantly, pyrrothiogatain treatment of $Cdc42^{Fllox/+}Foxp3^{YFP-Cre}$ mice restored tumor growth (figure 4K), correlating with reduced instability of tumor-infiltrating Treg cells and decreased tumor-infiltrating effector T cells (online supplemental figure 7A-D), indicating that heterozygous $Cdc42$ deletion induces Treg cell instability and revokes antitumor T-cell immunity attributable to GATA3 upregulation. Of note, inhibition of GATA3 in $Cdc42^{+/+}Foxp3^{YFP-Cre}$ Treg cells caused Treg cell instability (figure 4E-G and I,J), similar to that caused by the upregulation of GATA3 in $Cdc42^{Fllox/+}Foxp3^{YFP-Cre}$ Treg cells (figure 4B,C and E-G and I,J). And $Cdc42^{+/+}Foxp3^{YFP-Cre}$ mice treated with pyrrothiogatain showed tumor suppression, comparable to that in $Cdc42^{Fllox/+}Foxp3^{YFP-Cre}$ mice (figure 4K). The data suggest that physiological levels of GATA3 are critical for Treg cell stability and Treg cell-mediated tumor growth, mirroring CAI. As effector T cells and MC38 tumor cells from $Cdc42^{Fllox/+}Foxp3^{YFP-Cre}$ mice presumably express GATA3 at comparable levels to that from $Cdc42^{+/+}Foxp3^{YFP-Cre}$ mice, any direct effect of pyrrothiogatain on effector T cells and MC38 tumor cells is expected to affect tumor growth similarly in $Cdc42^{Fllox/+}Foxp3^{YFP-Cre}$ and $Cdc42^{+/+}Foxp3^{YFP-Cre}$ mice. In support, there was no change in GATA3 expression in tumor-infiltrating effector T cells from $Cdc42^{Fllox/+}Foxp3^{YFP-Cre}$ mice (data not shown). Thus, the differential effects of pyrrothiogatain on tumor growth in $Cdc42^{Fllox/+}Foxp3^{YFP-Cre}$ and $Cdc42^{+/+}Foxp3^{YFP-Cre}$ mice likely resulted from differential expression/DNA binding activity of GATA3 in $Cdc42^{Fllox/+}Foxp3^{YFP-Cre}$ and $Cdc42^{+/+}Foxp3^{YFP-Cre}$ Treg cells, reminiscent of acetazolamide.

We next examined how heterozygous $Cdc42$ deletion upregulates GATA3 in Treg cells. *Cdc42* functions through activating its immediate downstream effectors including WASP.²⁶ Similar to heterozygous $Cdc42$ deletion, genetic deletion of WASP has been shown to increase GATA3 expression in Treg cells.²⁷ Consistently, we found that treatment of Treg cells with a WASP inhibitor, wiskostatin,²⁸ enhanced the expression of GATA3 in a dose-dependent manner (figure 4L and online supplemental figure 7E). Furthermore, wiskostatin treatment upregulated CAI mRNA (figure 4M) and CAI protein (online supplemental figure 7F) and increased Treg cell instability (figure 4N,O). Consequently, inhibition of WASP by wiskostatin mimicked heterozygous $Cdc42$ deletion in eliciting antitumor T-cell immunity (figure 4P and online supplemental figure 7G-J). Collectively, these findings reveal that heterozygous $Cdc42$ deletion induces Treg cell instability to promote antitumor T-cell immunity

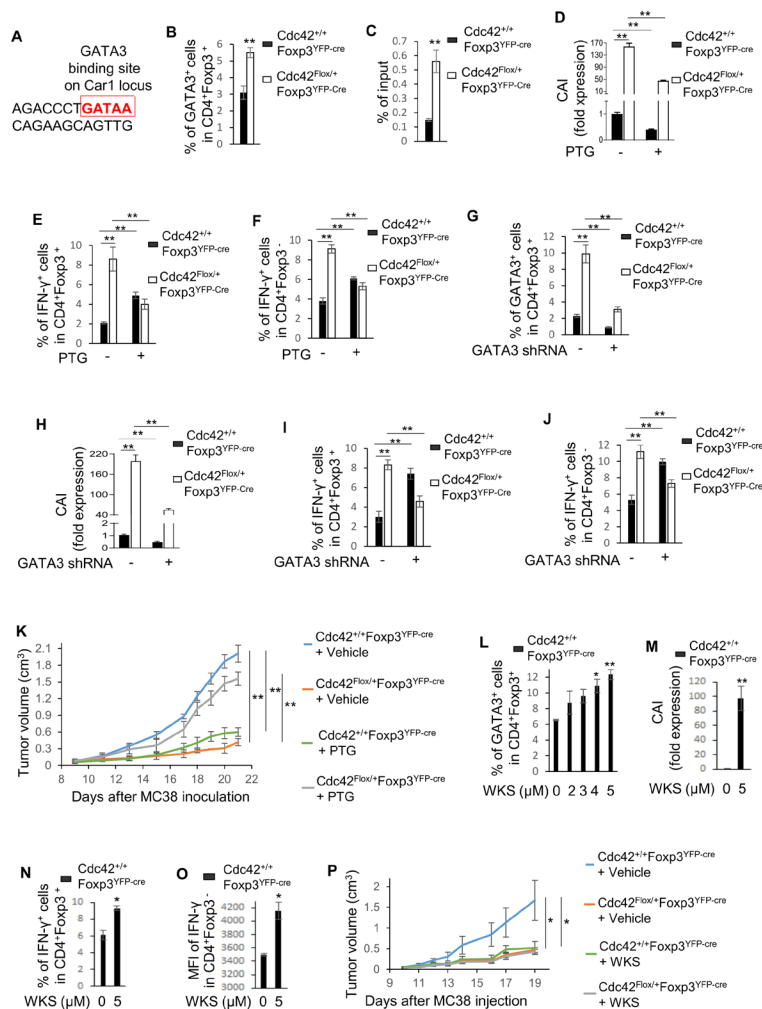


Figure 4 Heterozygous loss of *Cdc42* induces Treg cell instability and inhibits tumor growth through WASP-GATA3-mediated CAI expression. (A) Diagram of GATA3 binding sites on the CAI locus. (B) The percentages of GATA3⁺ cells in splenic Treg cells from *Cdc42*^{+/+}*Foxp3*^{YFP-Cre} and *Cdc42*^{Flox/+}*Foxp3*^{YFP-Cre} mice were analyzed by flow cytometry. (C) GATA3 binding to the CAI locus in splenic *Cdc42*^{+/+}*Foxp3*^{YFP-Cre} and *Cdc42*^{Flox/+}*Foxp3*^{YFP-Cre} Treg cells was analyzed by chromatin immunoprecipitation-quantitative real-time PCR. (D–F) Splenic *Cdc42*^{+/+}*Foxp3*^{YFP-Cre} and *Cdc42*^{Flox/+}*Foxp3*^{YFP-Cre} Treg cells were cultured for 3 days with PTG or vehicle. The expression of CAI mRNA was examined by quantitative real-time RT-PCR (D), The percentages of IFN-γ⁺ cells in Treg cells (E) and CD4⁺ effector T cells (ex-Treg) (F) were analyzed by flow cytometry. (G–J) Splenic *Cdc42*^{+/+}*Foxp3*^{YFP-Cre} and *Cdc42*^{Flox/+}*Foxp3*^{YFP-Cre} Treg cells were transduced with GATA3 shRNA or Scramble shRNA during 3 days' culture. The percentages of GATA3⁺ cells in Treg cells (G) and the percentages of IFN-γ⁺ cells in Treg cells (I) and CD4⁺ effector T cells (ex-Treg) (J) were analyzed by flow cytometry. The expression of CAI mRNA was analyzed by quantitative real-time RT-PCR (H). (K) *Cdc42*^{+/+}*Foxp3*^{YFP-Cre} and *Cdc42*^{Flox/+}*Foxp3*^{YFP-Cre} mice were inoculated with MC38 cells and treated with or without PTG at 60 mg/kg one time per day, starting at the same time as MC38 cell inoculation. Tumor volume was recorded. (L–O) Splenic *Cdc42*^{+/+}*Foxp3*^{YFP-Cre} Treg cells were cultured for 3 days with WKS or vehicle. The percentages of GATA3⁺ Treg cells (L) and the expression (percentages or MFI) of IFN-γ in Treg cells (N) and CD4⁺ effector T cells (ex-Treg) (O) were analyzed by flow cytometry. Of note, MFI of IFN-γ was analyzed in IFN-γ⁺ cells. The expression of CAI mRNA was analyzed by quantitative real-time RT-PCR (M). (P) *Cdc42*^{+/+}*Foxp3*^{YFP-Cre} and *Cdc42*^{Flox/+}*Foxp3*^{YFP-Cre} mice were inoculated with MC38 cells (1.4×10⁶) and treated with or without WKS at 60 mg/kg one time per day, starting at the same time as MC38 cell inoculation. Tumor volume was recorded. (B) Error bars indicate SD of four mice. (C) Error bars indicate SD of triplicates. Data are from eight mice pooled. (D–J and L–O) Error bars indicate SD of triplicates. Data are from five to six mice pooled. (K and P), Error bars indicate SD of four mice. Data are representative of two independent experiments. *p<0.05; **p<0.01. CAI, carbonic anhydrase I; IFN, interferon; GATA3, GATA transcription factor 3; mRNA, messenger RNA; PTG, pyrrothiogatain; MFI, mean fluorescence intensity; RT-PCR, reverse transcription polymerase chain reaction; Treg, regulatory T cells; WASP, Wiskott-Aldrich syndrome protein; WKS, wiskostatin.

through a WASP-GATA3-CAI signaling node. Of note, heterozygous *Cdc42* knockout Treg cells had <2fold increase in GATA3 expression (figure 4B) but ~12fold increase in CAI expression (figure 3A) and inhibition

of GATA3 in heterozygous *Cdc42* knockout Treg cells only partially reversed the increased CAI expression (figure 4D and H). The data suggest that *Cdc42* regulates CAI expression both dependent and independent of

GATA3. Along the same line, WASP-suppressed Treg cells had ~2fold increase in GATA3 expression (figure 4L) but >7fold increase in CAI expression (online supplemental figure 7F), suggesting that similar to *Cdc42*, WASP regulates CAI expression both dependent and independent of GATA3.

Pharmacological targeting of *Cdc42* triggers antitumor T-cell immunity through induction of Treg cell instability

To evaluate the potential of targeting *Cdc42* signaling as a cancer immunotherapy, we examined whether pharmacologic inhibition of *Cdc42* by a *Cdc42* activity-specific inhibitor, CASIN,¹⁷ could mimic heterozygous *Cdc42* deletion in inducing Treg cell instability without causing spontaneous systemic autoimmunity. In a previous study, we showed that treatment of C57BL/6 mice with 2.4 mg/kg of CASIN (i.p.) did not affect cell cycle progression of hematopoietic stem cells in bone marrow.¹⁷ Likewise, this dose of CASIN did not induce Treg cell instability (data not shown). However, while C57BL/6 mice treated with 30 mg/kg of CASIN two times a day for 1 week and then 40 mg/kg one time a day for another week did not show altered Treg cell homeostasis (online supplemental figure 8A), the mice had destabilized Treg cells, as evidenced by decreased Foxp3 expression in Treg cells (online supplemental figure 8B) and increased IFN- γ and/or IL-17 expression in Treg cells (online supplemental figure 8C) and effector T cells (online supplemental figure 8D, E). Intriguingly, the mice did not display weight loss (online supplemental figure 8F), tissue inflammation (online supplemental figure 8G) and increased autoantibodies (online supplemental figure 8H). Thus, at a certain treatment regimen, CASIN can mimic Treg cell-specific heterozygous *Cdc42* deletion.

Next, we prophylactically and therapeutically treated tumor-bearing mice with CASIN and found that CASIN effectively inhibited tumor growth (figure 5A and E), correlating with intratumoral Treg cell instability and increased effector T cells (figure 5B–D and F–H). Depletion of either CD4⁺ T/Treg cells by anti-CD4 neutralizing antibody or CD8⁺ T cells by anti-CD8 neutralizing antibody partially restored tumor growth in CASIN-treated mice (figure 5I, J), suggesting that the tumor suppression in CASIN-treated mice is due to both of the increased IFN- γ -producing CD4⁺ effector T/Treg cells and CD8⁺ effector T cells. To clarify whether CASIN directly increases CD4⁺ and CD8⁺ effector T cells to impact on tumor growth, we activated CD4⁺ and CD8⁺ T cells with anti-CD3/CD28 antibodies or tumor cells, in the presence or absence of CASIN at concentrations equivalent to the serum doses (~2–5 μ M) in therapeutic CASIN-treated tumor-bearing mice (online supplemental figure 9). We found that CASIN inhibited anti-CD3/CD28 or tumor cell-induced IFN- γ -producing CD4⁺ and CD8⁺ effector T cells (figure 5K–N). To examine whether CASIN inhibits effector T cells in vivo in tumor-bearing mice, we depleted Treg cells before tumor cell inoculation and CASIN treatment. We found that while Treg

cell depletion induced tumor suppression, CASIN treatment of Treg cell-depleted mice restored tumor growth, correlating with reduced tumor-infiltrating IFN- γ -producing CD4⁺ and CD8⁺ effector T cells (figure 5O–Q). Thus, it appears that on the one hand, CASIN destabilizes Treg cells, leading to increased effector T cells, and on the other hand, CASIN inhibits effector T cells in a cell-intrinsic manner. However, CASIN-induced increase in effector T cells through destabilizing Treg cells outweighs CASIN-induced autonomous decrease in effector T cells, resulting in a net increase in effector T cells and tumor suppression. Together, our data suggest that the increased effector T cells and tumor suppression in CASIN-treated mice are caused by Treg cell destabilization. To substantiate this, we treated tumor-bearing *Cdc42*^{Flox/+}*Foxp3*^{YFP-Cre} mice with CASIN and found that CASIN lost its inhibitory effect on tumor growth in *Cdc42*^{Flox/+}*Foxp3*^{YFP-Cre} mice (figure 5R), suggesting that CASIN does not poise off-target and off-Treg cell effects on tumor suppression. Moreover, we induced Treg cell instability ex vivo with CASIN (figure 6A and B) and then prophylactically (figure 6C) and therapeutically (figure 6I) transferred these Treg cells with congenic (CD45.1⁺) effector T cells into *Rag1*^{-/-} mice. We found that these CASIN-treated CD45.2⁺ Treg cells diminished tumor growth (figure 6D and J). There was a substantial increase in tumor-infiltrating effector T-cell cytokine-expressing Treg cells (figure 6E and K) and effector T cells that were converted from (figure 6F and L) or unleashed by (figure 6G, H, M and N) unstable Treg cells, suggesting that both the instability and the impaired suppressive function of Treg cells contribute to the tumor suppression in CASIN-treated mice, reminiscent of that in *Cdc42*^{Flox/+}*Foxp3*^{YFP-Cre} mice. Intriguingly, CASIN did not cause systemic autoimmunity in tumor-bearing mice (online supplemental figure 10), similar to that in tumor-free mice, further supporting that CASIN administration does not elicit off-target and off-Treg cell effects in suppressing tumor growth and allows for a therapeutic window for cancer treatment.

Although CASIN treatment of steady-state and tumor-bearing mice did not cause spontaneous inflammatory disorders, CASIN treatment of mice bearing DSS-induced colitis led to more weight loss, compared with vehicle treatment (online supplemental figure 11A). Consistent with an essential role of Th1 cells in the development of colitis,¹⁵ CASIN treatment increased the production of IFN- γ in colonic CD4⁺ effector T cells (online supplemental figure 11B). CASIN induced Treg cell instability in the colon, as evidenced by elevated IFN- γ ⁺ Treg cells (online supplemental figure 11C). Given our previous finding that CASIN did not enhance Th1 cell differentiation,²⁹ it is logical to reason that the increased IFN- γ ⁺ effector T cells are attributable to the Treg cell instability in CASIN-treated colitis-bearing mice. These results caution the use of CASIN in cancer patients who simultaneously suffer autoimmune diseases.

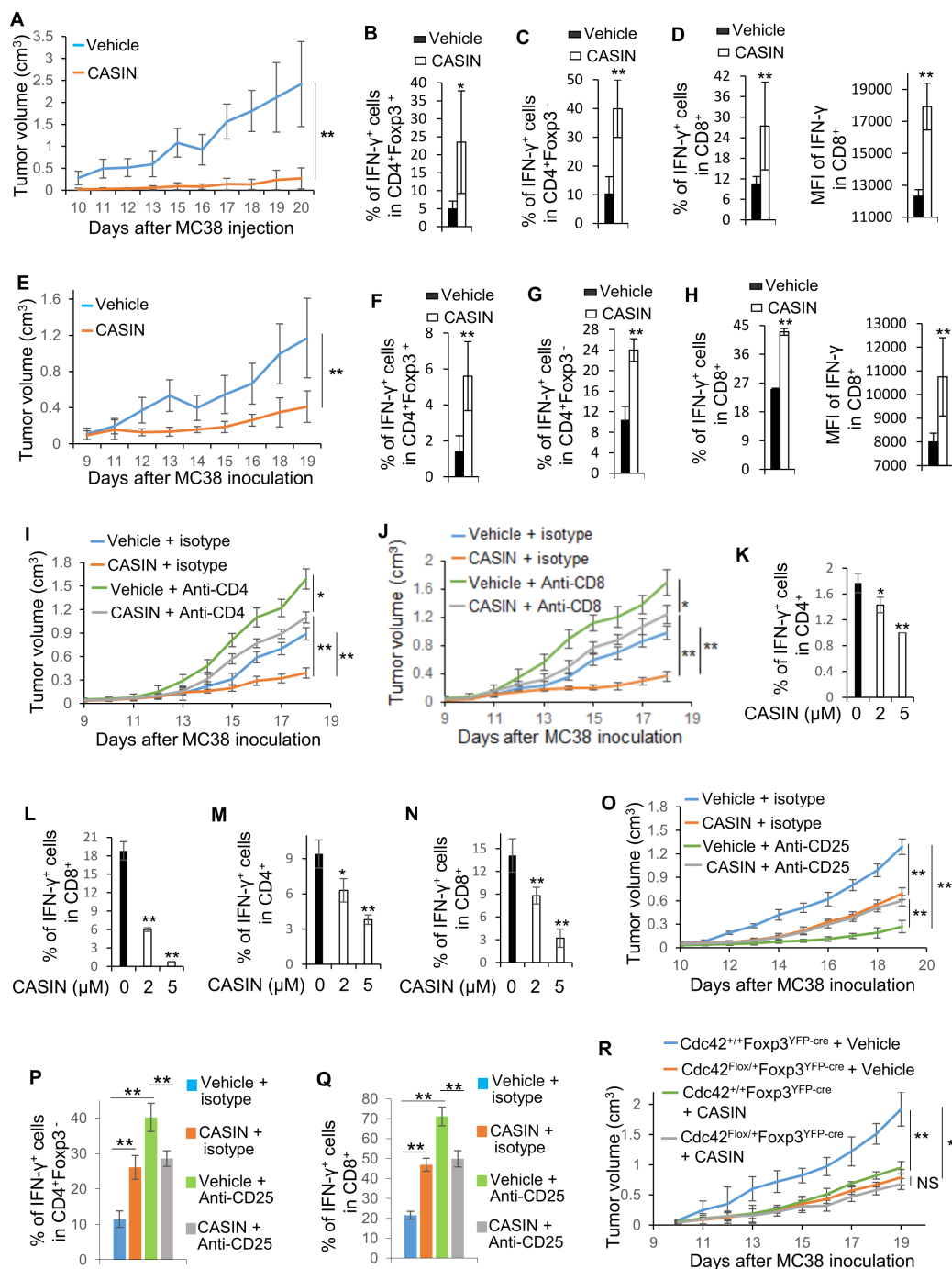


Figure 5 CASIN administration elicits antitumor T-cell immunity through Treg cell destabilization. (A–J) and (O–Q) C57BL/6 mice were inoculated with MC38 cells and injected with or without CASIN at 30 mg/kg two times a day for 7 days and then 40 mg/kg one time a day until the end of the experiment. CASIN injection was started either at the same time as MC38 cell inoculation (A–D) or on tumor onset (E–J). For T-cell depletion, anti-CD4 or anti-CD8 neutralizing antibody or isotype control was injected at 150 μ g/mouse for each antibody one time every other day for four injections and then two times a week until the end of the experiments. The injection was started at the same time as MC38 cell inoculation (I, J). For Treg cell depletion, anti-CD25 antibody or isotype control was injected at 500 μ g/mouse 1 day before MC38 cell inoculation (O–Q). Tumor volume was recorded (A, E, I, J, O). The expression (percentages and/or MFI) of IFN- γ in tumor-infiltrating Treg cells (B, F) and CD4⁺ (C, G, P) and CD8⁺ (D, H, Q) effector T cells was analyzed by flow cytometry. Of note, MFI of IFN- γ was analyzed in IFN- γ ⁺ cells. (K–N) Splenic Treg cell-depleted T cells from MC38 tumor-free (K, L) or tumor-bearing (M, N) C57BL/6 mice were cultured with anti-CD3/CD28 antibodies (K, L) or MC38 tumor cells at 2:1 ratio (M, N) for 3 days, in the presence or absence of CASIN. The cells were analyzed for IFN- γ expression in CD4⁺ (K, M) and CD8⁺ (L, N) T cells by flow cytometry. (R) *Cdc42^{Flox/+}Foxp3^{YFP-Cre}* and *Cdc42^{Flox/+}Foxp3^{YFP-Cre}* mice were inoculated with MC38 cells (1.4×10^6) and injected with or without CASIN, starting on tumor onset. Tumor volume was recorded. (A–H) Error bars indicate SD of six mice. (I, J, O–R) Error bars indicate SD of five mice. (K–N) Error bars indicate SD of triplicates. Data are from six mice pooled. Data are representative of two independent experiments. * $p < 0.05$; ** $p < 0.01$. IFN, interferon; MFI, mean fluorescence intensity; NS, no significance; Treg, regulatory T cells.

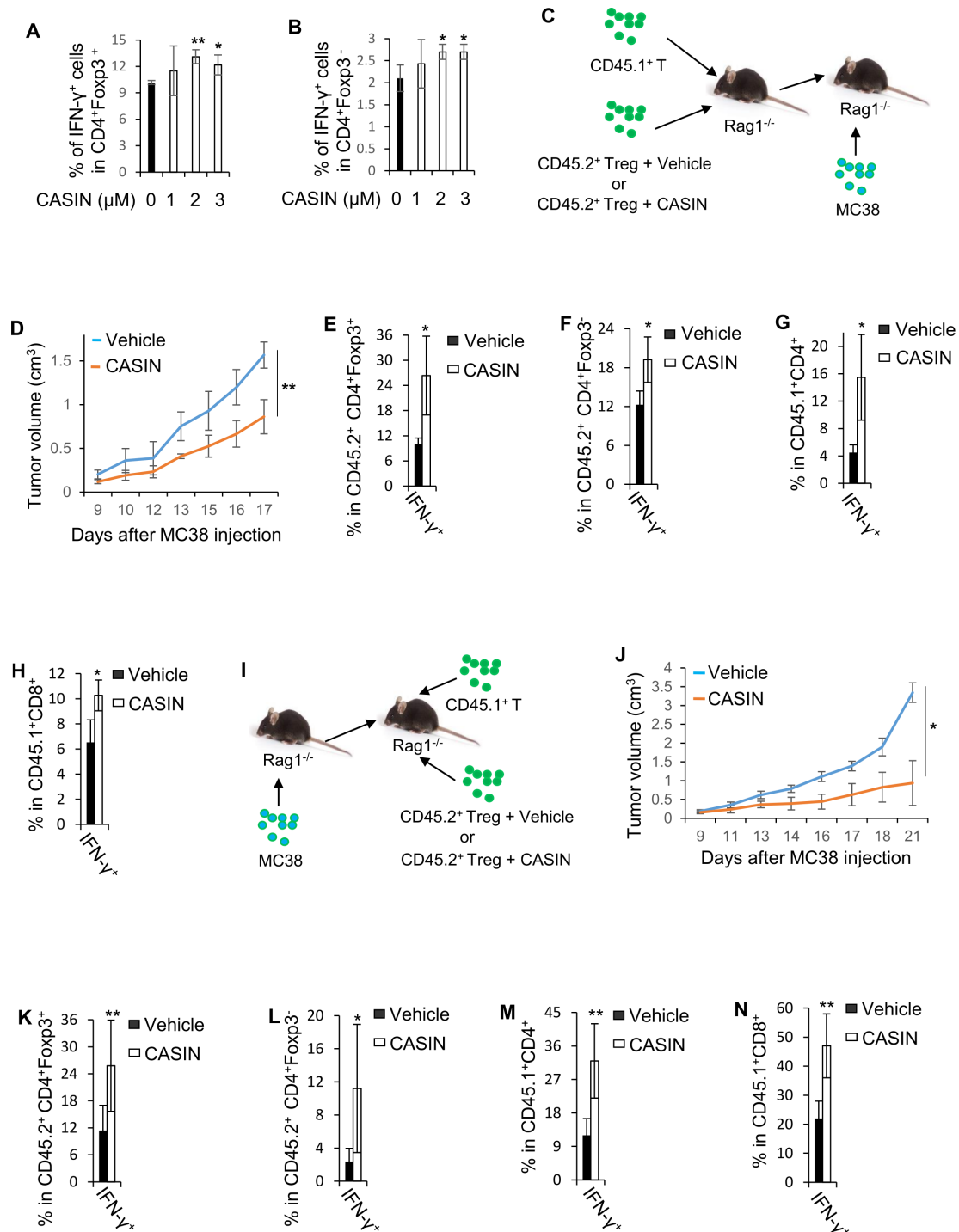


Figure 6 Treg cell instability induced ex vivo by CASIN treatment elicits antitumor T-cell immunity in vivo. (A, B) Splenic Treg cells from *Cdc42*^{+/+}*Foxp3*^{YFP-Cre} mice were treated with or without CASIN at the indicated concentrations for 3 days. The percentages of IFN- γ ⁺ cells in Treg cells (A) and CD4⁺ effector T cells (ex-Treg) (B) were analyzed by flow cytometry. (C–N) Treg cells treated with or without CASIN (2 μ M) were co-transferred with congenic T cells into Rag1^{-/-} mice either 1 day before (C) or 9 days after (on tumor onset) (I) MC38 cell inoculation. Tumor volume was recorded (D, J). The percentages of IFN- γ ⁺ cells in tumor-infiltrating Treg cells (E, K), ex-Treg cells (F, L), and congenic effector T cells (G, H, M, N) were analyzed by flow cytometry. (A, B) Error bars indicate SD of triplicates. Data are from five mice pooled. (D–H) Error bars indicate SD of four mice. (J–N) Error bars indicate SD of seven mice. **p*<0.05; ***p*<0.01. IFN, interferon; Treg, regulatory T cells.

Pharmacological targeting of *Cdc42* causes an additive effect on ICI-induced antitumor T-cell immunity

Although ICIs have achieved clinical success in several types of cancer, primary or acquired resistance in the

majority of patients with cancer limited their broad application.⁷ We thus examined whether CASIN can enhance ICIs' activity in tumor suppression. We found that combined CASIN and anti-PD-1 treatment inhibited

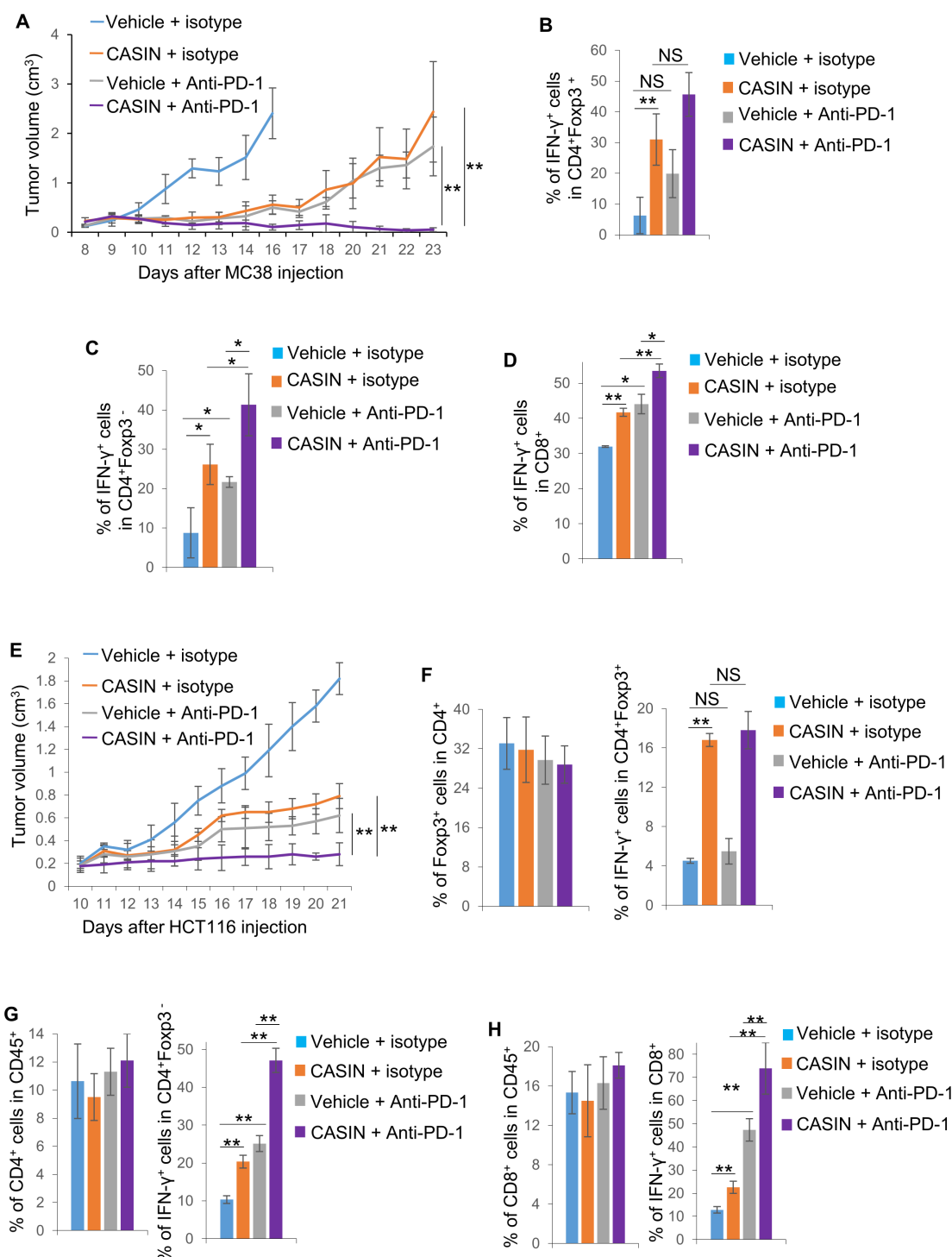


Figure 7 CASIN enhances anti-PD-1-induced antitumor T-cell immunity. C57BL/6 mice were inoculated with MC38 cells. On tumor onset, the mice were injected with or without CASIN (30 mg/kg two times a day for 7 days and then 40 mg/kg one time a day until the end of the experiment) and/or anti-PD-1 (150 µg/mouse every other day for five injections) (A–D). Alternatively, NSGS mice engrafted with CD34⁺ hematopoietic stem cells were inoculated with HCT116 cells (2×10^6) and treated with or without CASIN and/or anti-PD-1, on tumor onset (E–H). Tumor volume was recorded (A, E). The percentages of total and/or IFN-γ⁺ tumor-infiltrating Treg cells (B, F) and total and/or IFN-γ⁺ tumor-infiltrating CD4⁺ (C, G) and CD8⁺ (D, H) effector T cells were analyzed by flow cytometry. (A–D) Error bars indicate SD of three mice. (E–H) Error bars indicate SD of four mice. Data are representative of two independent experiments. * $p < 0.05$; ** $p < 0.01$. IFN, interferon; NS, no significance; PD-1, programmed cell death protein-1; Treg, regulatory T cells.

MC38 tumor growth to a greater extent than single treatment (figure 7A). Combined CASIN and anti-PD-1 treatment did not further increase Treg cell instability,

compared with CASIN alone (figure 7B). However, the combinatory treatment led to more IFN-γ-producing effector T cells (figure 7C,D), likely due to the ability

of anti-PD-1 to reinvigorate exhausted effector T cells. Moreover, compared with single treatment, combined CASIN and anti-PD-1 led to greater suppression of tumor growth of human colon cancer cells, HCT116, in mouse xenografts engrafted with human CD34⁺ hematopoietic stem cells (figure 7E). CASIN did not affect the frequency of tumor-infiltrating human Treg cells but induced their destabilization. Such instability was not further increased by the combinatory treatment (figure 7F). CASIN also did not affect the frequency of total human T cells in the tumor. However, it increased IFN- γ -producing human T cells. The combinatory treatment further increased IFN- γ -producing human T cells (figure 7G,H). Together, these results suggest that CASIN causes an additive effect on ICI-induced antitumor T-cell immunity.

DISCUSSION

In this study, we show that heterozygous deletion of *Cdc42*, inhibition of Cdc42 by CASIN and inhibition of Cdc42 immediate downstream effector WASP induce Treg cell instability, leading to antitumor T-cell immunity, suggesting that Cdc42-WASP is required for maintenance of Treg cell stability and tumor immune evasion. Mechanistically, Cdc42-WASP promotes Treg cell stability and tumor immune evasion through restraining a non-canonical signaling cascade, GATA3-CAI. Given that WASP can translocate to the nucleus to regulate gene transcription in Th1 cells,³⁰ it is plausible that in Treg cells, Cdc42 promotes nuclear translocation of WASP, leading to inhibition of GATA3 transcription. Upregulation of intracellular CAI in heterozygous *Cdc42* knockout Treg cells causes alkalization of extracellular pH, suggesting that CAI-induced HCO₃⁻ is transported into extracellular space. Such alkalization of extracellular pH can induce Treg cell instability, enabling effector T cells to fight against tumor growth. Our future study is aimed at determining the mechanism underlying alkalization of extracellular pH-induced Treg cell instability. We speculate that extracellular alkaline is detected by alkali-sensing receptors (eg, InsR-RR)³¹ that in turn elicit intracellular signals to promote DNMT3a expression and thus methylation of *CNS2* of the *Foxp3* locus, leading to loss of stable *Foxp3* expression and subsequent derepression of effector T-cell cytokine (eg, IFN- γ) expression.

Of note, the frequencies of IL-4⁺ Treg cells and effector T cells are increased in steady-state but not tumor-bearing heterozygous *Cdc42* knockout mice. On the other hand, the frequencies of IFN- γ ⁺ Treg cells and effector T cells are increased in tumor-bearing but not steady-state heterozygous *Cdc42* knockout mice. Likewise, the frequencies of IFN- γ ⁺ Treg cells and effector T cells are increased on *in vitro* culture of heterozygous *Cdc42* knockout Treg cells. Thus, it appears that the effect of heterozygous deletion of *Cdc42* on Treg cell instability phenotypes is context-dependent. It is conceivable that in steady-state heterozygous *Cdc42* knockout mice, CAI-induced Treg cell extracellular pH alkalization, which is demonstrated

in culture, is partially offset by an unknown mechanism, leading to mild instability phenotypes. As tumor-bearing but not steady-state heterozygous *Cdc42* knockout mice show increased CD8⁺ effector T cells, we envision that unstable heterozygous *Cdc42* knockout Treg cells lose their suppressive activity toward effector T cells in tumor bearing but not steady-state heterozygous *Cdc42* knockout mice. In support, in tumor-bearing *Rag1*^{-/-} mice that are co-transferred with CD45.2⁺ heterozygous *Cdc42* knockout Treg cells and CD45.1⁺ effector T cells, CD45.1⁺ effector T cells are derepressed. Since tumor-bearing *Rag1*^{-/-} mice that are transferred with heterozygous *Cdc42* knockout Treg cells alone show Treg cell conversion to effector T cells, we reason that in tumor-bearing heterozygous *Cdc42* knockout mice, Treg cell instability phenotypes are reflected by both conversion to effector T cells and loss of suppressive function. In contrast, in steady-state heterozygous *Cdc42* knockout mice, Treg cell instability phenotypes are reflected by conversion to effector T cells only.

Inhibition of CAI or GATA3 at least partially restores Treg cell stability in heterozygous *Cdc42* knockout Treg cells and tumor immune evasion in heterozygous *Cdc42* knockout mice. In contrast, inhibition of CAI or GATA3 dampens Treg cell stability in Cdc42-proficient Treg cells and tumor immune evasion in Cdc42-proficient mice. Although it remains elusive why inhibition of CAI or GATA3 causes opposite effects in heterozygous *Cdc42* knockout Treg cells or mice to that in Cdc42-proficient Treg cells or mice, our data demonstrate that both increased and decreased CAI and GATA3 in Treg cells can cause Treg cell instability and antitumor T-cell immunity, suggesting that physiologic levels of CAI and GATA3 are important for maintaining Treg cell stability and its mediated tumor immune evasion. Our findings are reminiscent of that physiological levels of glycolysis are essential for maintaining Treg cell stability, as indicated by that either high glycolysis in *pTEN* knockout Treg cells²¹ or low glycolysis in *Cdc42* homozygous knockout Treg cells¹⁵ is associated with Treg cell instability.

We have reported that homozygous *Cdc42* deletion in Treg cells decreases Treg cell numbers, induces Treg cell instability, and causes systemic inflammatory disorders.¹⁵ Here we show that heterozygous *Cdc42* deletion also induces Treg cell instability with an increase in methylation of *CNS2* of the *Foxp3* locus and a concomitant decrease in *Foxp3* expression comparable to that induced by homozygous *Cdc42* deletion. However, heterozygous *Cdc42* deletion does not alter Treg cell homeostasis and cause spontaneous autoimmunity. Thus, it is logical to reason that the autoimmune responses in homozygous *Cdc42* knockout mice are primarily caused by dampened Treg cell homeostasis. Interestingly, at a certain regimen, CASIN treatment mimics heterozygous but not homozygous *Cdc42* deletion in modulating Treg cells. Importantly, similar to heterozygous *Cdc42* deletion, CASIN treatment does not trigger autoimmune diseases. It is noteworthy mentioning that while Treg cell instability induced by heterozygous *Cdc42* deletion or CASIN

is moderate in steady-state mice, the instability phenotypes are magnified in the TME, which are able to cause tumor suppression in tumor-bearing heterozygous *Cdc42* knockout or CASIN-treated mice. These findings support the notion that the dosage effect of *Cdc42* expression/activity in Treg cells can be harnessed to unleash anti-tumor T-cell immunity without causing autoimmunity. In further support, we show that CASIN treatment does not appear to have off-target and off-Treg cell effects on tumor suppression, which is corroborated by that CASIN treatment of heterozygous *Cdc42* knockout mice does not cause additive effect to *Cdc42* heterozygosity in tumor suppression, nor does it cause systemic inflammation in tumor-bearing mice. It is conceivable that CASIN treatment of heterozygous *Cdc42* knockout mice further decreases *Cdc42* activity in heterozygous *Cdc42* knockout Treg cells. Nevertheless, CASIN at the dose/kinetics used in our study does not further inhibit tumor growth in heterozygous *Cdc42* knockout mice. The data suggest that any additional reduction in *Cdc42* activity in Treg cells from CASIN-treated heterozygous *Cdc42* knockout mice is not sufficient to cause additive Treg cell instability and tumor suppression. Noting that CASIN selectively inhibits *Cdc42* in a dose-dependent manner,¹⁷ it is possible that an increased dosage/frequency of CASIN treatment causes more profound tumor suppression in heterozygous *Cdc42* knockout mice. However, such regimen of CASIN may also cause autoimmunity, mimicking Treg cell-specific homozygous loss of *Cdc42*.¹⁵ In these contexts, certain regimens of *Cdc42* inhibitors are expected to be effective and have manageable toxicity. Finally, *Cdc42* is known to promote tumorigenesis^{32–34} and thus a *Cdc42* inhibitor may have tumor cell-intrinsic effect in suppressing tumor growth. Nonetheless, the complete restoration of tumor growth by T-cell depletion in CASIN-treated mice indicates that the immuno-effect outweighs any tumor cell-intrinsic effect, suggesting that oncogenic *Cdc42* may serve as an immunotherapeutic target. Collectively, our findings suggest that targeting of *Cdc42*-regulated Treg cell stability may be a valuable addition to the current cancer immunotherapies that only benefit a small proportion of patients with cancer.

Author affiliations

¹Division of Experimental Hematology and Cancer Biology, Children's Hospital Medical Center, and Department of Pediatrics, University of Cincinnati College of Medicine, Cincinnati, Ohio, USA

²Division of Allergy and Immunology, Children's Hospital Medical Center, and Department of Pediatrics, University of Cincinnati College of Medicine, Cincinnati, Ohio, USA

³Division of Biomedical Informatics, Children's Hospital Medical Center, and Department of Pediatrics, University of Cincinnati College of Medicine, Cincinnati, Ohio, USA

Contributors KK initiated, performed and analyzed the experiments, and wrote the manuscript. J-QY performed and analyzed the experiments. MW prepared the NSGS mice engrafted with CD34+ human hematopoietic stem cells. VM performed and analyzed the experiments. PN performed the experiments. YL performed the experiments. TW analyzed the RNA sequencing (RNA-seq) data. AKD analyzed the RNA-seq data. RV performed the experiments. QRL designed the experiments. AGJ analyzed the transcription factor binding sites on the carbonic anhydrase I locus.

YZ conceived the study, supervised the project, and designed the experiments, and wrote the manuscript. FG conceived the study, supervised the project, designed and analyzed the experiments, and wrote the manuscript. FG acts as guarantor.

Funding This work was supported in part by grants from the National Institutes of Health (R01GM108661 to FG, R56 HL141499 to FG, R01CA234038 to FG and YZ, and R50CA211404 to MW) and from the Cincinnati Children's Hospital Medical Center (RIP funding to FG).

Competing interests None declared.

Patient consent for publication Not applicable.

Ethics approval Not applicable.

Provenance and peer review Not commissioned; externally peer reviewed.

Data availability statement All data relevant to the study are included in the article or uploaded as supplementary information.

Supplemental material This content has been supplied by the author(s). It has not been vetted by BMJ Publishing Group Limited (BMJ) and may not have been peer-reviewed. Any opinions or recommendations discussed are solely those of the author(s) and are not endorsed by BMJ. BMJ disclaims all liability and responsibility arising from any reliance placed on the content. Where the content includes any translated material, BMJ does not warrant the accuracy and reliability of the translations (including but not limited to local regulations, clinical guidelines, terminology, drug names and drug dosages), and is not responsible for any error and/or omissions arising from translation and adaptation or otherwise.

Open access This is an open access article distributed in accordance with the Creative Commons Attribution Non Commercial (CC BY-NC 4.0) license, which permits others to distribute, remix, adapt, build upon this work non-commercially, and license their derivative works on different terms, provided the original work is properly cited, appropriate credit is given, any changes made indicated, and the use is non-commercial. See <http://creativecommons.org/licenses/by-nc/4.0/>.

ORCID iDs

Ashley Kuenzi Davis <http://orcid.org/0000-0003-1162-3994>

Fukun Guo <http://orcid.org/0000-0002-8820-7633>

REFERENCES

- 1 Finn OJ. A believer's overview of cancer immunosurveillance and immunotherapy. *J Immunol* 2018;200:385–91.
- 2 Ribas A, Wolchok JD. Cancer immunotherapy using checkpoint blockade. *Science* 2018;359:1350–5.
- 3 Sharma P, Hu-Lieskovan S, Wargo JA, et al. Primary, adaptive, and acquired resistance to cancer immunotherapy. *Cell* 2017;168:707–23.
- 4 Ohkura N, Kitagawa Y, Sakaguchi S. Development and maintenance of regulatory T cells. *Immunity* 2013;38:414–23.
- 5 Dang EV, Barbi J, Yang H-Y, et al. Control of T(H)17/T(reg) balance by hypoxia-inducible factor 1. *Cell* 2011;146:772–84.
- 6 Gomez-Rodriguez J, Wohlfert EA, Handon R, et al. Itk-mediated integration of T cell receptor and cytokine signaling regulates the balance between Th17 and regulatory T cells. *J Exp Med* 2014;211:529–43.
- 7 Liu M, Guo F. Recent updates on cancer immunotherapy. *Precis Clin Med* 2018;1:65–74.
- 8 Nishikawa H, Sakaguchi S. Regulatory T cells in cancer immunotherapy. *Curr Opin Immunol* 2014;27:1–7.
- 9 Shitara K, Nishikawa H. Regulatory T cells: a potential target in cancer immunotherapy. *Ann N Y Acad Sci* 2018;1417:104–15.
- 10 Byrne WL, Mills KHG, Lederer JA, et al. Targeting regulatory T cells in cancer. *Cancer Res* 2011;71:6915–20.
- 11 Colamattéo A, Carbone F, Bruzzaniti S, et al. Molecular mechanisms controlling FOXP3 expression in health and autoimmunity: from epigenetic to post-translational regulation. *Front Immunol* 2019;10:3136.
- 12 Takahashi R, Nishimoto S, Muto G, et al. SOCS1 is essential for regulatory T cell functions by preventing loss of Foxp3 expression as well as IFN- γ and IL-17A production. *J Exp Med* 2011;208:2055–67.
- 13 Zheng Y, Josefowicz S, Chaudhry A, et al. Role of conserved non-coding DNA elements in the *Foxp3* gene in regulatory T-cell fate. *Nature* 2010;463:808–12.
- 14 Melendez J, Grogg M, Zheng Y. Signaling role of *Cdc42* in regulating mammalian physiology. *J Biol Chem* 2011;286:2375–81.
- 15 Kalim KW, Yang J-Q, Li Y, et al. Reciprocal regulation of Glycolysis-Driven Th17 pathogenicity and regulatory T cell stability by *Cdc42*. *J Immunol* 2018;200:2313–26.

- 16 Parkkila S. Significance of pH regulation and carbonic anhydrases in tumour progression and implications for diagnostic and therapeutic approaches. *BJU Int* 2008;101:16–21.
- 17 Liu W, Du W, Shang X, *et al.* Rational identification of a Cdc42 inhibitor presents a new regimen for long-term hematopoietic stem cell mobilization. *Leukemia* 2019;33:749–61.
- 18 Wunderlich M, Chou F-S, Sexton C, *et al.* Improved multilineage human hematopoietic reconstitution and function in NSGS mice. *PLoS One* 2018;13:e0209034.
- 19 Teng MWL, Swann JB, von Scheidt B, *et al.* Multiple antitumor mechanisms downstream of prophylactic regulatory T-cell depletion. *Cancer Res* 2010;70:2665–74.
- 20 Zhao C, Deng Y, Liu L, *et al.* Dual regulatory switch through interactions of TCF7L2/TCF4 with stage-specific partners propels oligodendroglial maturation. *Nat Commun* 2016;7:10883.
- 21 Huynh A, DuPage M, Priyadharshini B, *et al.* Control of PI(3) kinase in Treg cells maintains homeostasis and lineage stability. *Nat Immunol* 2015;16:188–96.
- 22 Li X, Liang Y, LeBlanc M, *et al.* Function of a FOXP3 cis-element in protecting regulatory T cell identity. *Cell* 2014;158:734–48.
- 23 Wei G, Abraham BJ, Yagi R, *et al.* Genome-Wide analyses of transcription factor GATA3-mediated gene regulation in distinct T cell types. *Immunity* 2011;35:299–311.
- 24 Wang Y, Su MA, Wan YY. An essential role of the transcription factor GATA-3 for the function of regulatory T cells. *Immunity* 2011;35:337–48.
- 25 Nomura S, Takahashi H, Suzuki J, *et al.* Pyrrothiogatain acts as an inhibitor of GATA family proteins and inhibits Th2 cell differentiation in vitro. *Sci Rep* 2019;9:17335.
- 26 Guo F, Hildeman D, Tripathi P, *et al.* Coordination of IL-7 receptor and T-cell receptor signaling by cell-division cycle 42 in T-cell homeostasis. *Proc Natl Acad Sci U S A* 2010;107:18505–10.
- 27 Lexmond WS, Goettel JA, Lyons JJ, *et al.* FOXP3+ Tregs require WASP to restrain Th2-mediated food allergy. *J Clin Invest* 2016;126:4030–44.
- 28 Kim H, Falet H, Hoffmeister KM, *et al.* Wiskott-Aldrich syndrome protein (WASP) controls the delivery of platelet transforming growth factor- β 1. *J Biol Chem* 2013;288:34352–63.
- 29 Yang J-Q, Kalim KW, Li Y, *et al.* Rational targeting Cdc42 restrains Th2 cell differentiation and prevents allergic airway inflammation. *Clin Exp Allergy* 2019;49:92–107.
- 30 Sadhukhan S, Sarkar K, Taylor M, *et al.* Nuclear role of WASP in gene transcription is uncoupled from its ARP2/3-dependent cytoplasmic role in actin polymerization. *J Immunol* 2014;193:150–60.
- 31 Brown D, Wagner CA. Molecular mechanisms of acid-base sensing by the kidney. *J Am Soc Nephrol* 2012;23:774–80.
- 32 Sakamori R, Yu S, Zhang X, *et al.* CDC42 inhibition suppresses progression of incipient intestinal tumors. *Cancer Res* 2014;74:5480–92.
- 33 Arias-Romero LE, Chernoff J. Targeting Cdc42 in cancer. *Expert Opin Ther Targets* 2013;17:1263–73.
- 34 Porter AP, Papaioannou A, Malliri A. Deregulation of Rho GTPases in cancer. *Small GTPases* 2016;7:123–38.